REFLECTION IMAGING OF DEEP STRUCTURE BENEATH SOUFRIERE HILLS VOLCANO, MONTSERRAT USING MICROEARTHQUAKE SOURCES

A Thesis

Presented to the Faculty of the Graduate School

of Cornell University

In Partial Fulfillment of the Requirements for the Degree of

Master of Science

by

Katrina Marie Byerly

May 2010

ABSTRACT

The SEA-CALIPSO experiment, carried out in December, 2007, was designed to image structure related to active volcanism beneath the island of Montserrat in the Caribbean. As part of that experiment, over 209 “Texan” recorders with 5 Hz geophones were deployed in 3 linear arrays at a nominal spacing of 100m, primarily to record signals from an airgun source towed offshore around the island. One goal of this controlled source experiment was to probe for magma and related structure using reflected phases from the airguns. However, the wide-angle geometries imposed by topography and bathymetry greatly limited the effectiveness of this approach. Fortunately, because the recorders were operating in continuous mode for three days, a number of shallow microearthquakes under the active summit of Soufriere Hills Volcano (SHV) were also recorded. Of the approximately 20 events that were recorded, only 7 had small enough error in the location to be used individually in our analysis and 14 had location errors small enough to be considered for stacking. Here we report results of processing those recordings as multichannel CMP (common midpoint) reflection sources, with emphasis on careful statics corrections and coherency enhancement. The data indicate the presence of subhorizontal reflectors at depths between 6 and 19km, which we interpret as sill complexes emplaced beneath SHV. The results of this analysis suggest that densely spaced (< 100m) arrays recording natural events in volcanic regions are a viable and less expensive alternative to controlled source surveys, especially where access is severely restricted near active volcanic centers.

BIOGRAPHICAL SKETCH

Katrina received her Bachelors of Science degree in geophysics from the University of South Carolina (USC) in May 2007. While there, she took an active role in leadership of the undergraduate geology club, planning trips to see geology in other regions of the country and world and organizing other activities. She also was dedicated to educational outreach, going to different afterschool programs to talk to students about geology for several weeks out of the year. While these opportunities were influential, undergraduate research had a much bigger impact on Katrina's career as a student. Upon her arrival at USC, she almost immediately began working with Dr. Tom Owens and had the privilege of working with him all four years of her undergraduate degree. Her main research project used receiver functions to look at the crustal structure and extent of delamination beneath the Sierra Nevada Mountains in California. As a senior, Katrina received an honorable mention in the NSF Graduate Research Fellowship Program.

Katrina came to Cornell University in 2007 and received a second honorable mention in the NSF Graduate Research Fellowship Program. Although all her research had been in earthquake seismology through this point, she was very interested in learning more about volcano seismology. She had the opportunity to be part of the field work portion of an active source seismic experiment conducted on Montserrat to image Soufriere Hills volcano. Katrina has enjoyed using microearthquakes recorded during this experiment to look for reflections beneath the island.

Upon completion of this Masters degree, Katrina will work as a seismologist in Brisbane, Australia.

This thesis is dedicated to my parents, Richard and Kathy Byerly, who were always there to encourage me and constantly praying for me.

ACKNOWLEDGMENTS

First and foremost, I want to give thanks to Jesus Christ, my Savior and my God, for creating this awesome world that I have the privilege of learning more about. Without His everlasting mercy, I would not be where I am today.

I would like to thank my advisor, Larry Brown, for giving me the opportunity to work on the SEA-CALIPSO project. Larry provided me with countless ideas and support while I was working on my thesis. I would also like to thank my other committee member, Rowena Lohman, for her input and willingness to help. This research was funded by the Continental Dynamics Program of the National Science Foundation (Grant No. EAR-060772).

I'm also very grateful for my lab and officemates, Chen, Tiffany, Danielle, and Naomi, for being willing to listen and provide encouragement when I needed it. I would also like to to thank the entire SEA-CALIPSO research team for their contributions in the field and in discussion.

Lastly, I want to thank my Ithaca GCF family because without their constant prayers and fellowship, life in Ithaca would have been much more difficult: Neela for always being there with a hug; Jen for all the haircuts and fun times together; Alvina and Heidi for encouraging my silliness; Phil for letting me adopt him as an older brother and Bekah for being a totally awesome sister; Jen, Jon, Nicole and Geoff for all the rock climbing fun times; Tim and Steve for introducing me to a new world of board games; Heather for introducing me to more veggies and giving me opportunities to work in her garden; everyone who was willing to eat something I made even though it was fried or ridiculously sweet. There are so many others that have provided good conversations and lots of laughs that I could not begin to list everyone, so here is where I'll stop.

TABLE OF CONTENTS

LIST OF FIGURES

LIST OF TABLES

Introduction

Volcanic eruptions have widespread economic, environmental, and humanitarian consequences for modern society. Our understanding about volcanoes and their magma systems is important so we can share information about the risks with the general public. One way we can increase our knowledge about volcanoes is by imaging their sub-surface structure. Seismic analysis, using both man-made and earthquake sources, is an important tool that can help scientists assess volcanic hazards and image the underlying magma chamber of a volcano. In this thesis, I have examined the use of both airgun sources and microearthquake sources for the imaging of the active volcano, Soufriere Hills, on the island of Montserrat. I am approaching the data using standard multichannel reflection imaging techniques for both the airgun sources and the microearthquake sources. While this is a typical procedure for working with active source data, earthquake data is rarely looked at in this manner because appropriate instrumentation is rarely fortuitously located in the areas affected by a particular earthquake.

Montserrat

Montserrat is a small island located in the northern part of the Lesser Antilles island arc. The island arc was formed by the ongoing subduction of the North American plate beneath the Caribbean plate at a current rate of approximately 2cm/yr. The island is about 16 km from north to south and 10km east to west. There are three regions of volcanic activity on the island: Silver Hills, Centre Hills and Soufriere Hills (from north to south) and seven volcanic centers total (Figure 1).

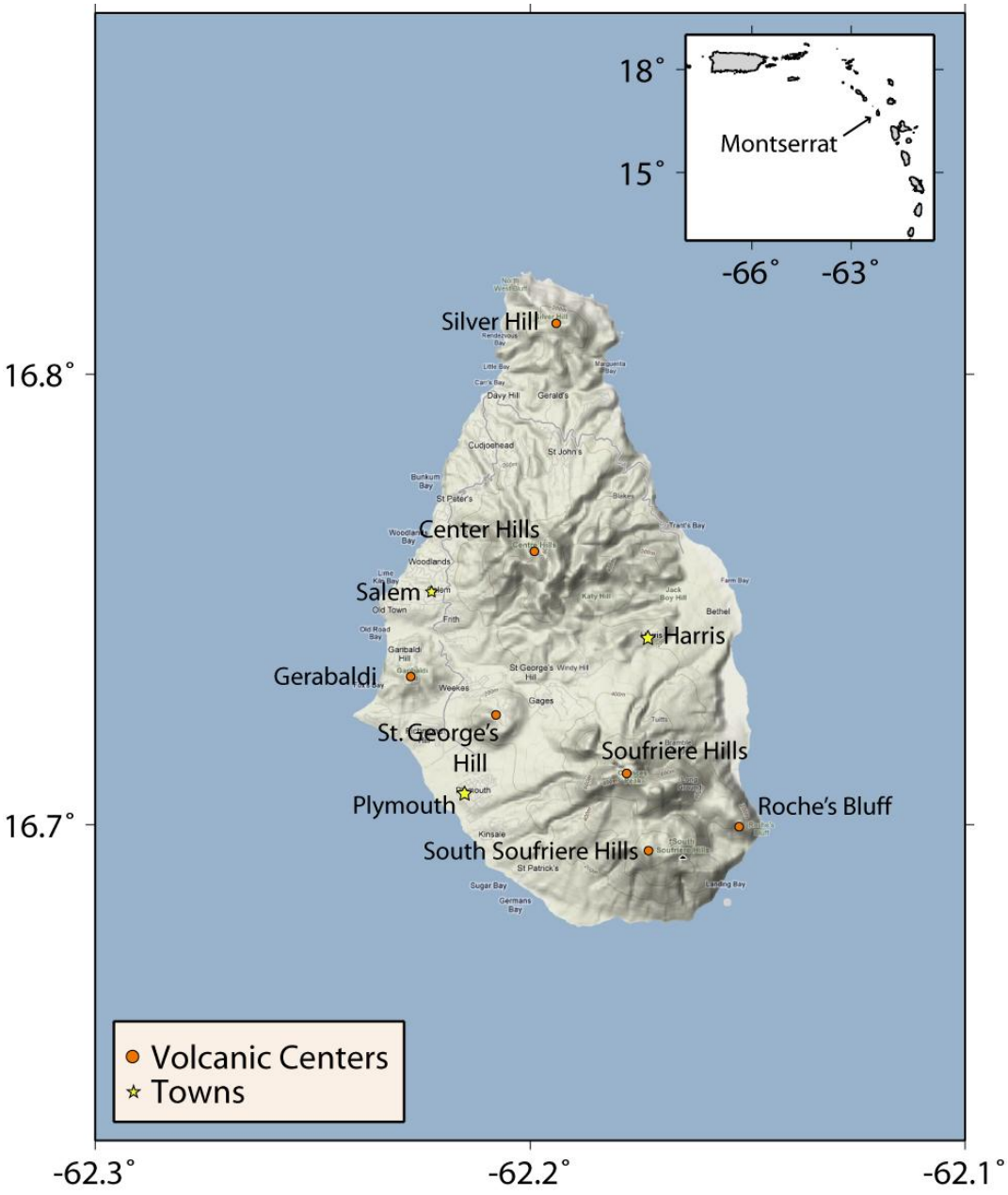

Figure 1 - Terrain map of Montserrat showing the locations of the volcanic centers, and important places.

Early observations concluded that age of volcanic activity became younger as you moved further south on the island based on differences in the amount of erosion each region had undergone (Davis, 1926). More recent work has dated the volcanism using K-Ar geochronology and confirmed this observation. Silver Hills is the oldest volcanic region and is in the northernmost part of the island. Volcanic activity occurred *c*. 2600 to *c*. 1200 ka and the andesitic lava that makes up Silver Hills has been heavily eroded (Harford *et al.* 2002). Centre Hills are in the center of the island and the rocks there have also undergone a great deal of erosion. Volcanic activity at Centre Hills dates from *c*. 950 to *c*. 550ka (Harford *et al.* 2002). Soufriere Hills Volcano (SHV) is located on the southern half of the island and is the volcano that is currently active. Based on dating done by Harford *et al.* (2002), volcanism began at SHV *c*. 170 ka. The last major eruption occurred ~300 years ago but there have been periods of minor activity since.

Modern Eruption of Soufriere Hills Volcano

The current eruption at Soufriere Hills Volcano began in July 1995 and has involved four eruptive phases of dome building separated by periods of quiescence (Elsworth *et al.*, 2008). The first eruptive phase occurred July 1995 to March 1998, the second spanned November 1999 to July 2003, and the third phase began in August 2005 and ended in March. Between each of these phases there was a period of reduced activity. The eruptive phases can be characterized by cycles of andesitic dome building, followed by dome collapses along with pyroclastic flows, lahars and vulcanian explosions. Seismic activity has been a major factor in the eruption with precursory earthquakes beginning three years before the current eruption began. There

were also periods of increased seismicity in 1897-1898, 1933-1937, and 1966-1967, none of which resulted in an eruption (Shepherd *et al.* 1971).

Montserrat and Soufriere Hills have been studied in great detail since the beginning of the most recent eruption to learn more about the associated magma system. Geochemical analysis of erupted andesites suggests that the magma is being stored in a chamber at a depth of at least 5-6 km (Barclay et al., 1998). The distribution of hypocenters of local earthquakes implies that any large magma chamber must be at a depth greater than 5km (Aspinall et al., 1998). A magma chamber modeled using a 1km average radius and 6km depth best explains the observed ground deformation (Mattioli et al., 1998). One interpretation using both magma flux data and ground deformation is that there are two magma chambers with a larger chamber at 12km feeding a smaller chamber at 6km (Elsworth et al., 2008).

SEA-CALIPSO

Anomalously strong reflections, or “bright spots”, have been identified from deep seismic reflection surveys around the world. Most of these bright spots have been interpreted as being due to magma, with the large amplitudes attributed to liquid material in juxtaposition with solid country rock. Examples of such “magma” bright spots include the Socorro Bright Spot (Brown *et al.*, 1979), the Death Valley Bright Spot (DeVoogd *et al*., 1986) and the Tibetan Bright Spots (Brown *et al*., 1996). Amplitude anomalies attributable to deep magmatism have also been recognized on teleseismic converter imagery (receiver functions) at an increasing number of locations around the world (e.g. Sheetz and Schlue, 1992, Chmielowski *et al*., 2003). The prominent expression of magma as a reflection/conversion on these relatively high

resolution seismic techniques was one inspiration for the SEA-CALIPSO experiment conducted on Montserrat.

The SEA-CALIPSO (Seismic Experiment with Airgun-source - Caribbean Andesitic Lava Island Precision Seismo-geodetic Observatory) experiment was designed to provide a better image of the deep structure beneath Soufriere Hills and to further the understanding of the active volcanic system using seismic data. The project consisted of two main elements, an earthquake seismology part and an on-shore off-shore active source seismic experiment. In October, 2007, 28 three component seismometers were deployed on the island to record both teleseismic and regional earthquakes. The active source component of the SEA-CALIPSO experiment was carried out in December 2007 with the deployment of 10 ocean bottom seismometers (OBS) and 209 Texans (Figure 2).

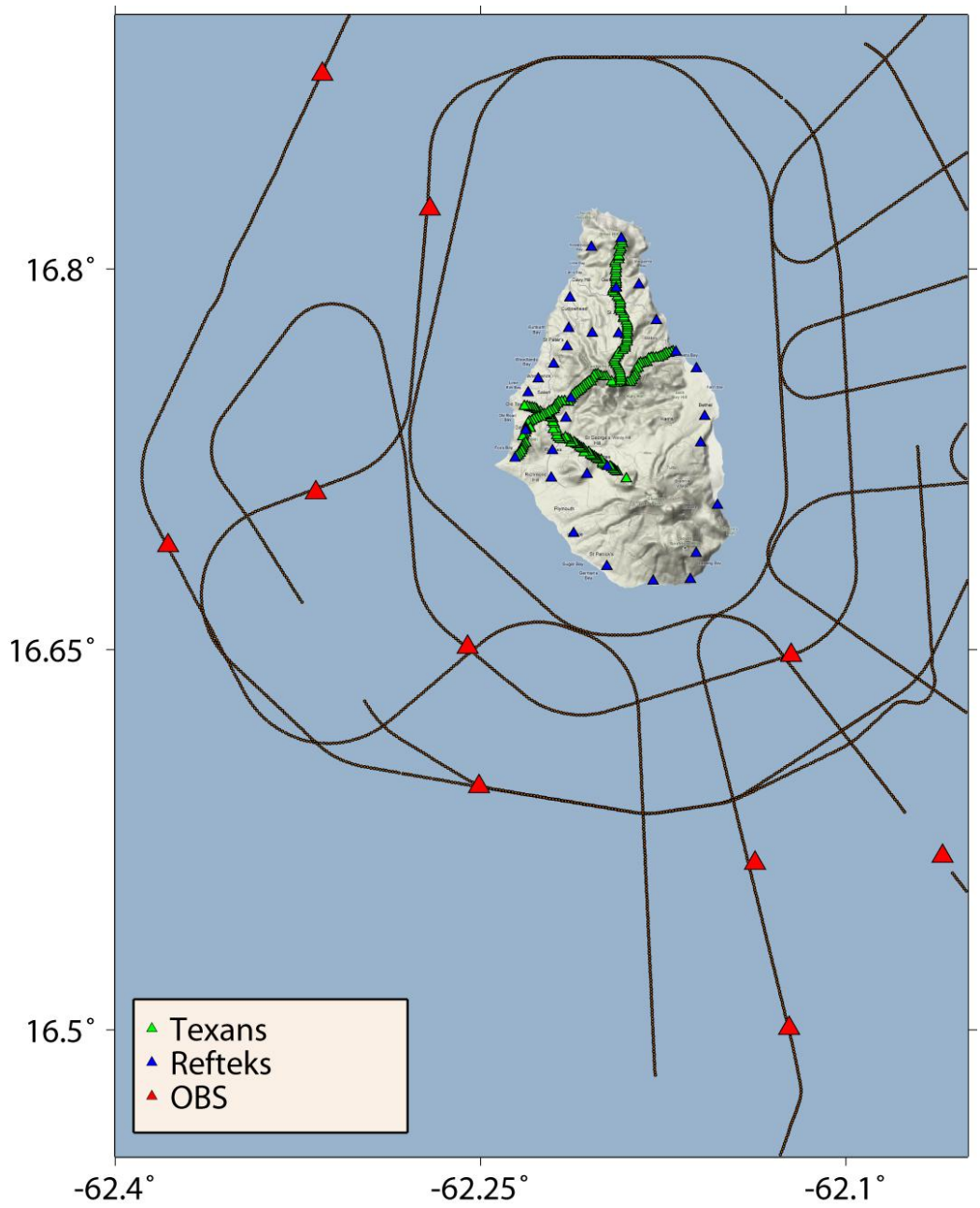

Figure 2 - Map showing the SEA-CALIPSO ship track and the locations of the one component seismometers (Texans), three component seismometers (RT 130), and ocean bottom seismometers (OBS).

The small size of the island and the ongoing volcanic activity at Montserrat made it an attractive location for an on-shore off-shore seismic experiment. The focus of this thesis is the recordings made by the dense reflection spreads consisting of 209 Texans recorders equipped with 5Hz geophones. These deployments constituted three lines (Figure 2), two radiating NW and N from SHV and the third providing "fan" coverage for sources on and SE of SHV. These arrays were designed in part to "undershoot" SHV with airgun sources on the RSS James Cook. Continuous, as opposed to windowed, recording was used because of nature of the airgun source (one shot every 60 seconds).

Survey Design Considerations

In order to guide the interpretation of the experimental results, we created a nominal velocity model and calculated synthetic seismograms from it using a Crewes finite difference code. The upper 10km of the model used to calculate the synthetic receiver gather, is based on a tomographic cross-section(A to A' in Figure 3), computed by Paulatto (2010, Figure 4) from the SEA-CALIPSO data. Because there was no ray coverage deeper than ~10km (Paulatto, 2010), we assumed a uniform lower crustal velocity down to the Moho at a depth of 30km (Figure 5). The Moho depth was based on receiver functions calculated from teleseismic data recorded on seismic stations located on Montserrat that show the Moho at a depth of ~30km (Sevilla *et al*., 2008). In our model we emplaced two hypothetical sills, which are positioned so a larger, deeper magma chamber is feeding a smaller, shallower magma chamber as suggested by Elsworth (2008).

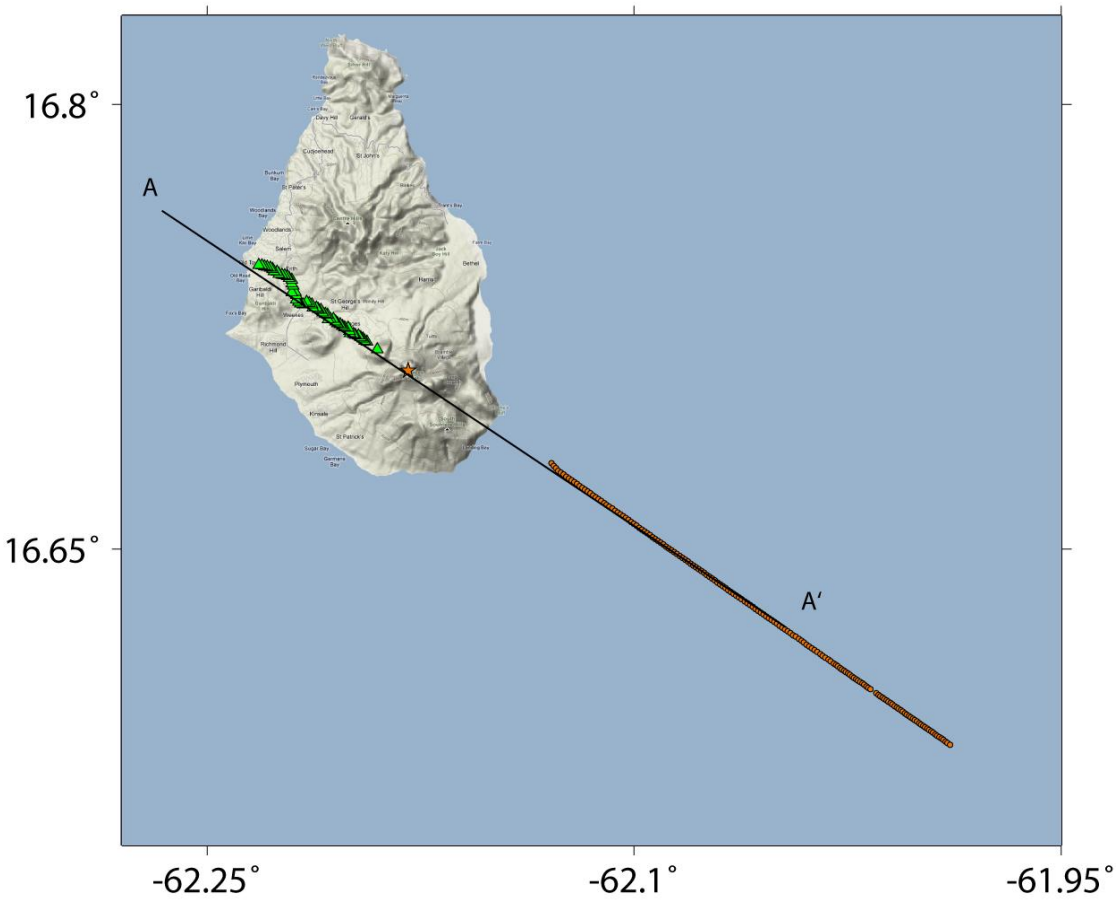

Figure 3 - Map showing Belham Valley stations (green triangles), SHV (orange star), and radial line of airgun shots (orange circles). A to A' is the line along which the tomographic cross-section and our synthetics are located.

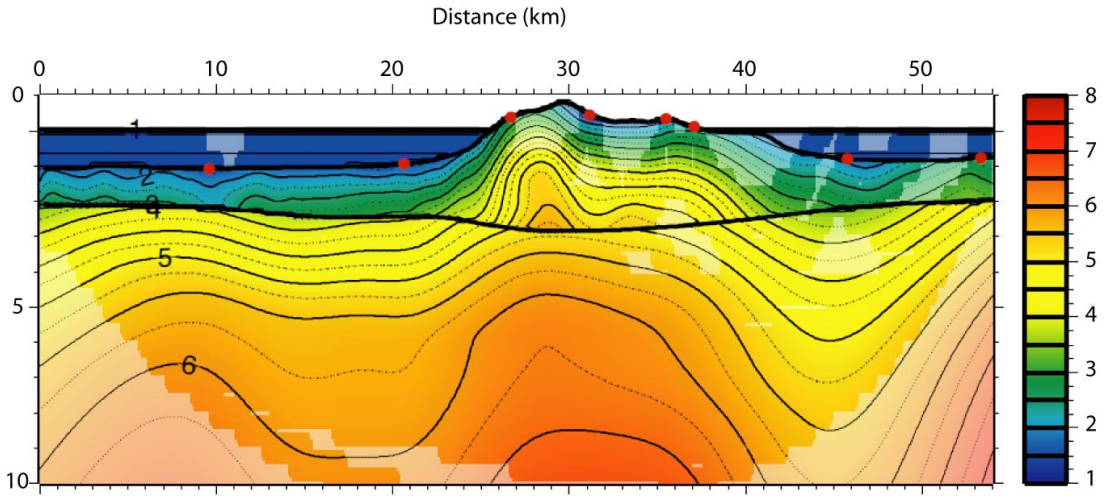

Figure 4 - Velocity model from Paulatto *et al*., 2010. This cross-section is approximately located along A to A' in Figure 3. Paler areas are not sampled by rays inverted in the final step.

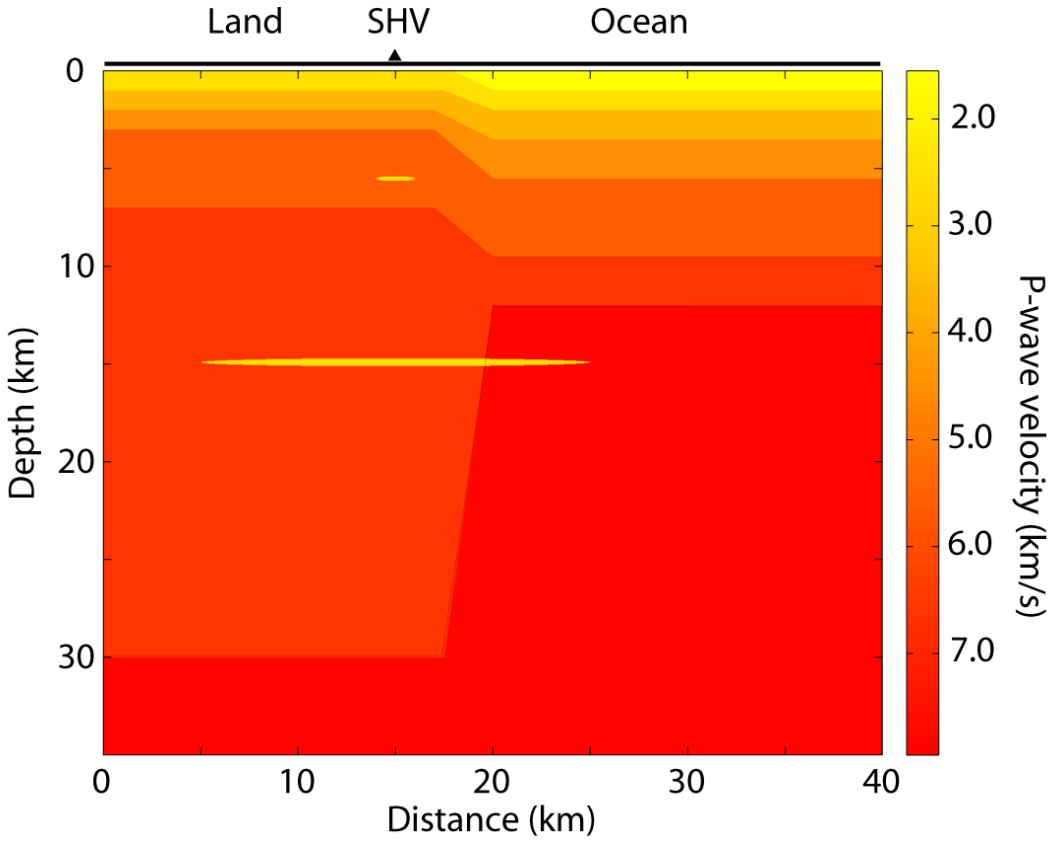

Figure 5 - Velocity model representing a receiver (or source) near SHV and sources (or receivers) every 100m along A to A' in Figure 3.

A receiver was placed directly above SHV and traces were generated for shots along a line with spacing every 100m and the resulting receiver gather is shown in Figure 7. The reflections from shallow structure beneath SHV are easily identified due to their distinct hyperbolic shape at the closer offsets (i.e. 0-5km from the receiver) (Figure 6). The deeper sill is also easily identified by a strong amplitude event, while the shallower sill is not as obvious due to the close proximity of reflections from the shallow structure (Figure 6).

Offsets for the airgun data range from approximately 7 to 25km along a radial line of shots for the closest Belham Valley receiver to SHV (Figure 3),

and optimal source-receiver offset along this line is about 7-12km. This is the region between the red lines in Figure 6. The synthetic data at these offsets show reflections from the shallow crustal structure that are asymptotic to the stronger direct arrivals, making it difficult to distinguish between the direct arrivals and reflections from shallow crustal layers (Figure 7). The distinguishing feature of reflections from deeper structure is the different apparent velocity relative to the direct refracted arrivals (Figure 7). However, these deeper reflections are obscured to some degree by energy from earlier arrivals and multiples.

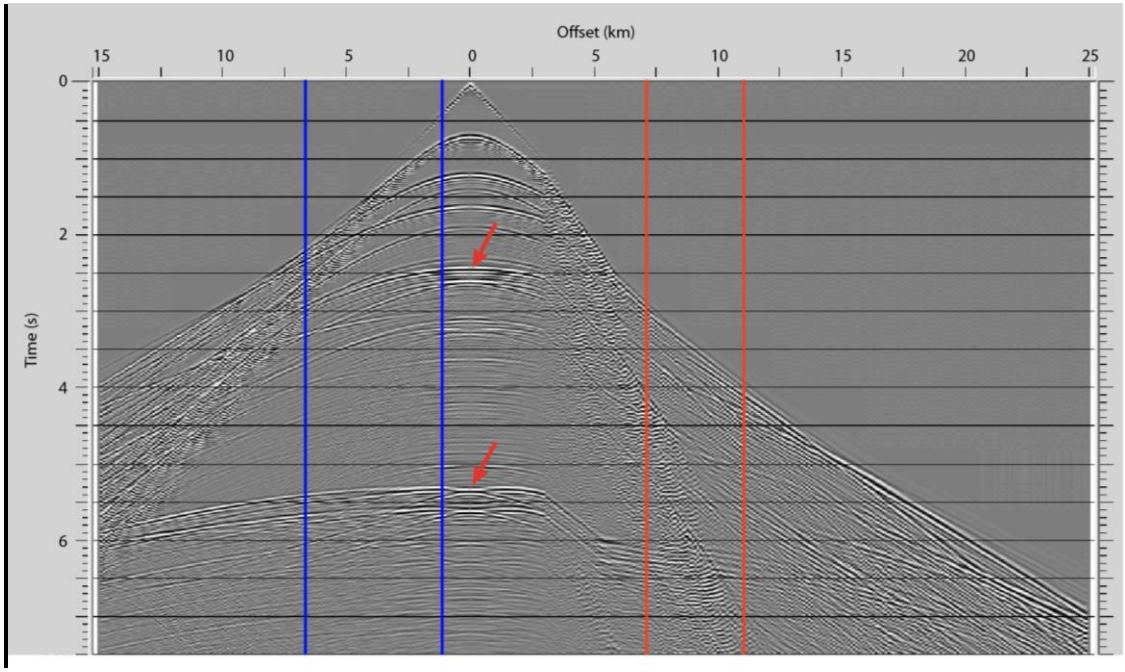

Figure 6 - Synthetic receiver gather for the velocity model. Area between red lines corresponds to offsets for a receiver near SHV and sources off-shore. Area between blue lines corresponds to offsets for a source near SHV and the Belham Valley receivers. Red arrows correspond to the reflections from the sills

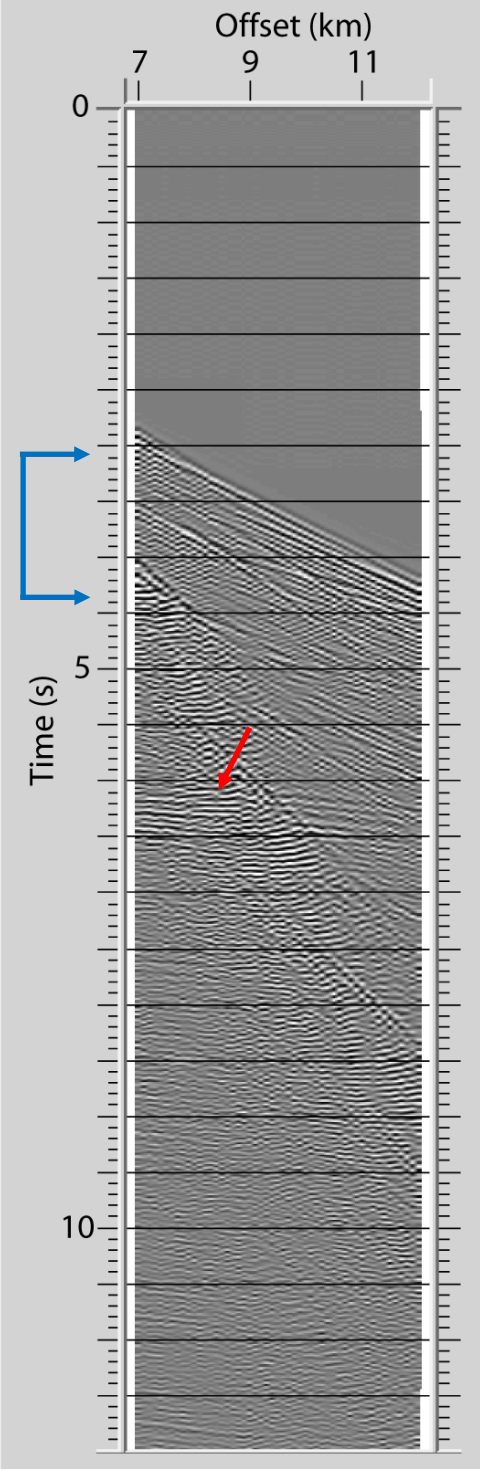

Figure 7 – Synthetic receiver gather for closest offsets along the Belham Valley line. This is the area between the red lines in Figure 6. Red arrow indicates arrival from the deep sill, blue arrows indicate arrivals from shallow layering

Results from the Airgun Recording

Approximately 4,414 shots were recorded by the Texans during the course of the experiment. There were several major challenges in using the shot data for seismic reflection analysis. One of the biggest issues with using the shots specifically for looking at the structure beneath Montserrat and the Soufriere Hills Volcano is that, because of the distance between the ship and the island, the majority of the offsets between the sources and receivers were so large that the majority of the reflection positions (common midpoints , or CMPs) were not actually under the island at all, and those under the island were typically not under SHV (Figure 8).

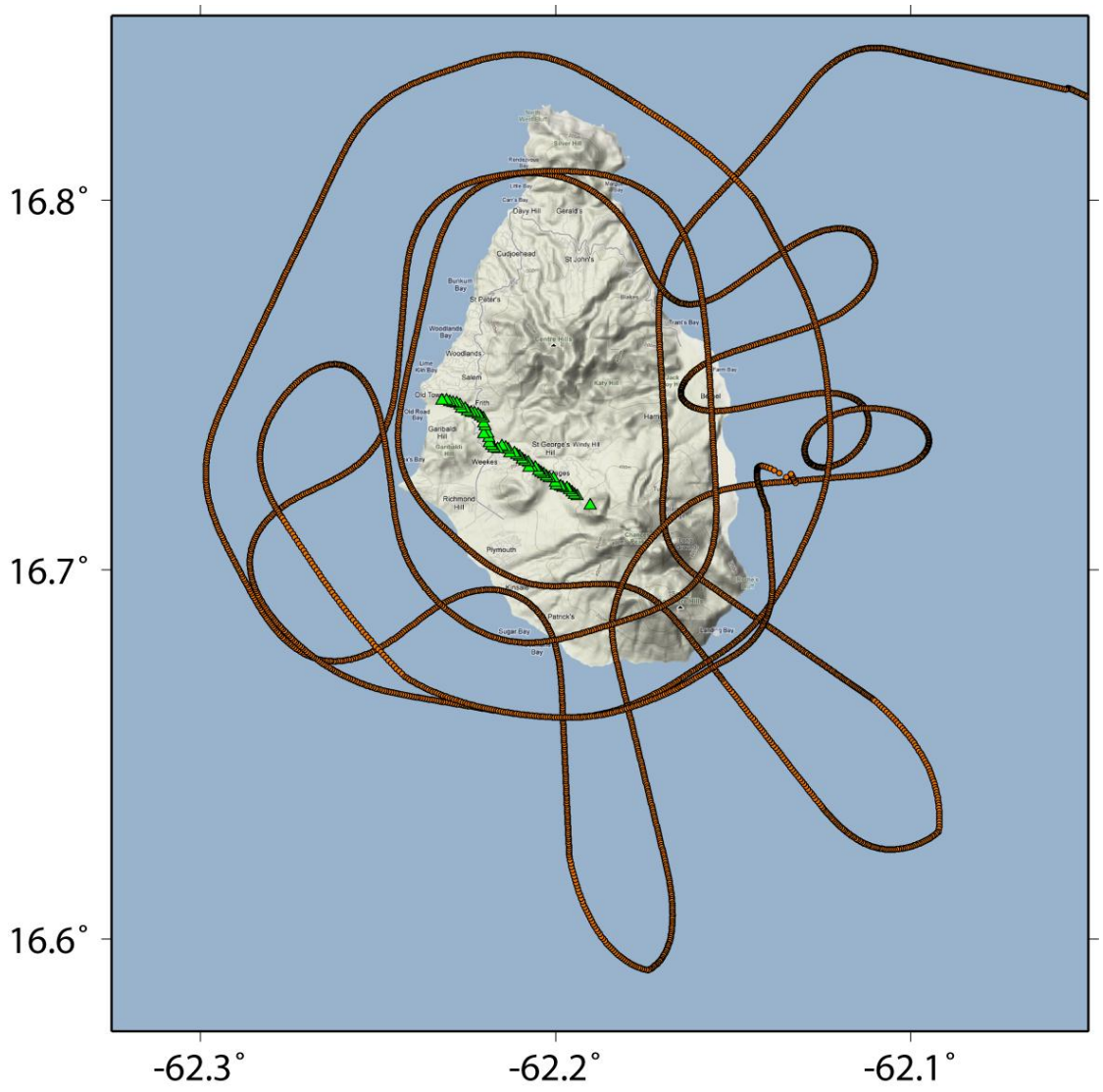

Figure 8 - Map showing the Belham Valley line (green triangles) and all the CMPs from the airgun shots (orange dots).

Another issue was that the shallowest structure beneath the island (e.g. less than 7 km) was not imaged due to the wide angle geometry of the survey. Additionally, multiples from the ocean floor obscured most of the data as seen in the receiver gathers in Figure 9. In many cases it is difficult to distinguish between the multiples and true reflections because everything appeared to be linear, while the multiples would normally have a different moveout from the

true reflections. There were also other arrivals, e.g. the direct water wave, further obscuring possible deep reflections (Figure 10). A stack of the data, which combines all the traces with a common midpoint in order to increase the signal to noise ratio, should have improved the data by stacking together reflections and canceling out the background noise. However, a stack for the Belham Valley stations along a radial line did not seem to make the data any more coherent (Figure 11). Due to the wide-angle offset, there is no data above 9km and the majority of the data is offshore. The only coherent energy under the island has apparent velocities corresponding to those that would be expected for multiples of the direct wave or the water wave. There is also a possible reflector about 12km from SHV at a depth of 32km.

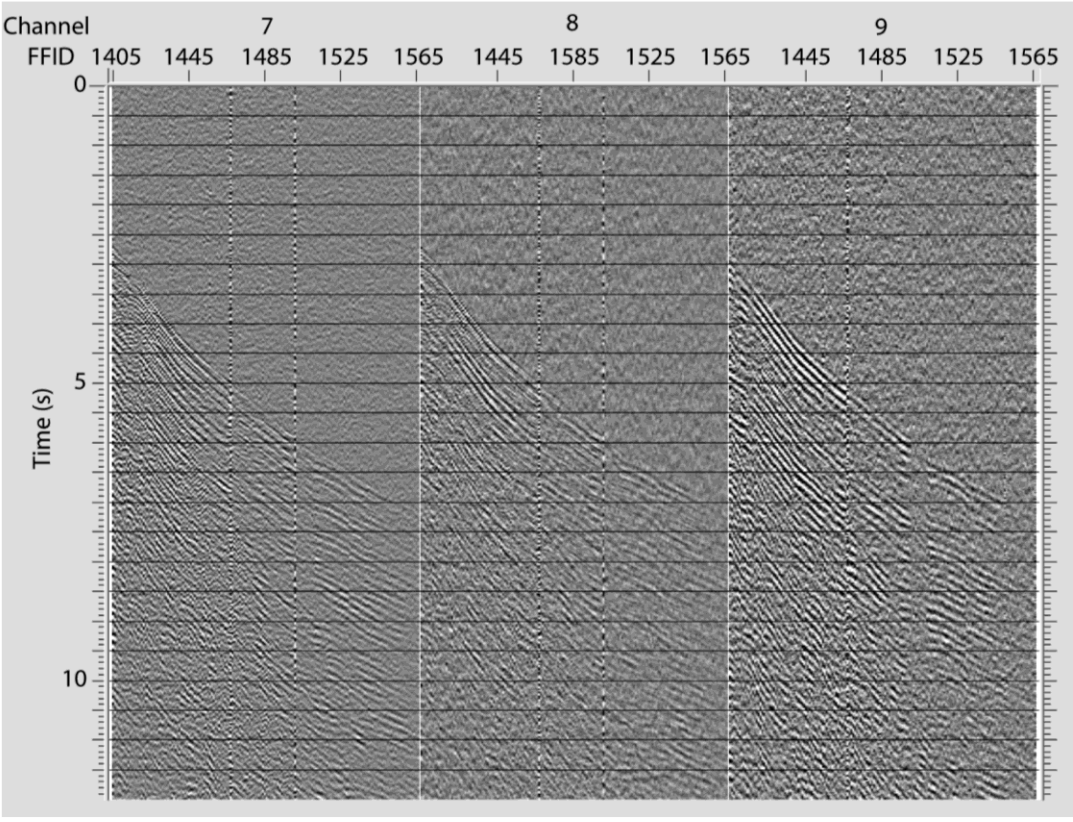

Figure 9 - Typical receiver gathers for the Belham Valley line.

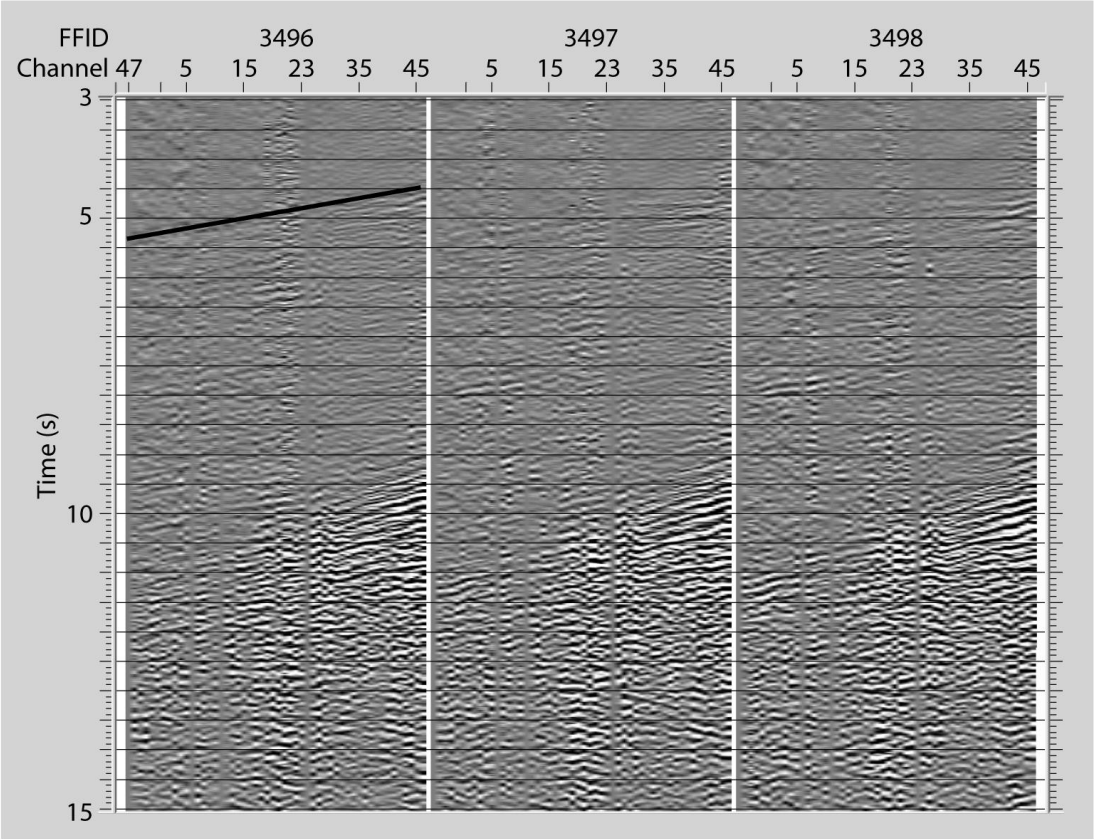

Figure 10 - Typical shot gather data from the Belham Valley line. The black line indicates the direct arrival.

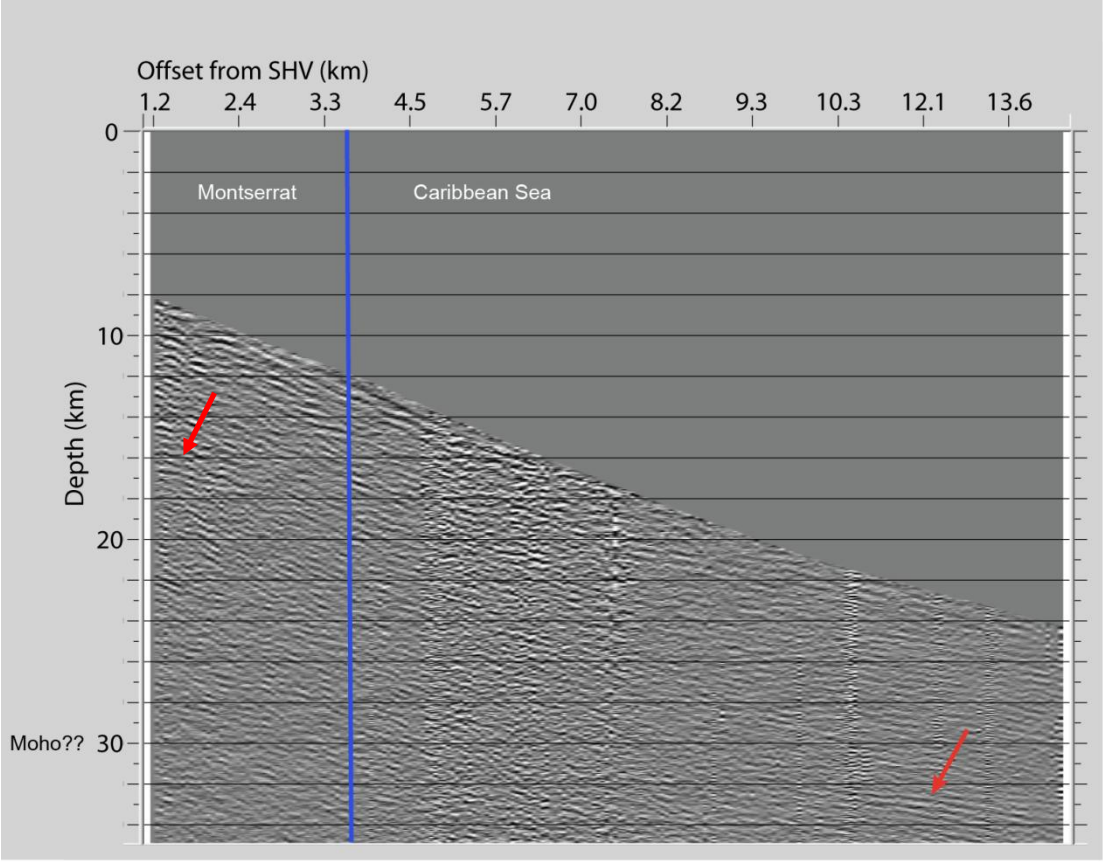

Figure 11 - Stack along the Belham Valley radial line. The blue line marks the edge of the island and the red arrows point out possible reflections

Earthquakes sources

The airgun data as a whole has proven disappointing in terms of mapping reflectivity. This leads us to consider other sources. We can switch the roles of sources and receivers, so the velocity model we used at earlier can also be used to compute a source gather for a source located beneath SHV and with receiver every 100m (Figure 5). If the source was located beneath SHV, the Belham Valley receivers would now be at offsets from 1.5-7km (Figure 6). Because shorter offsets are involved, this synthetic shot

gather exhibits clear reflections from the shallow layers (Figure 12). The reflection from the deeper sill is not obscured by reverberations and is much easier to identify. A source beneath SHV would also allow imaging under the island as opposed to mostly imaging off-shore, which is the case with the airgun shots. Fortunately we have sources near SHV in the form of microearthquakes.

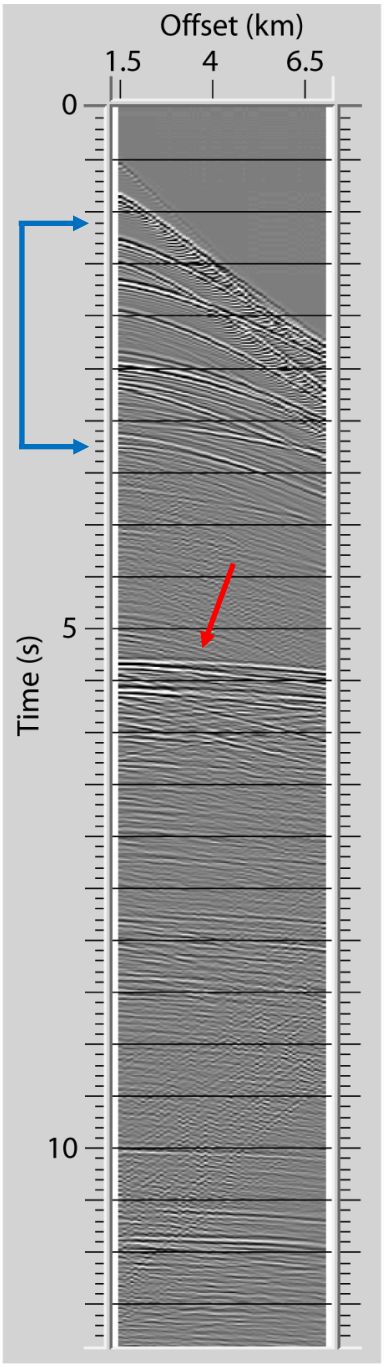

Figure 12 – Synthetic shot gather for offsets similar to a source being beneath SHV and the Belham Valley receivers. This is the area between the blue lines in Figure 6. Red arrow indicates arrival from the deep sill, blue arrows indicate arrivals from shallow layering.

Reflections from crustal discontinuities identified on microearthquake seismograms have provided critical evidence of magma at depth at a number of sites around the world. Sanford and Long (1965) first reported a midcrustal shear wave reflector beneath the Rio Grande Rift near Socorro, New Mexico, that was subsequently interpreted as an extensive magma sill (e.g. Sanford *et al.*, 1973; Sanford *et al*., 1977) . The distribution of such reflecting points suggests a lateral extent of at least 3400 km^2 for the magma body (Balch *et al*., 1997). Microearthquake recordings have been used in Japan to identify anomalous S-wave reflectors, likewise interpreted as magma bodies, beneath several volcano complexes, typically at depths less than 20km (e.g. Hasegawa *et al.*, 1991; Inamori *et al.*, 1992; Iidaka *et al.*, 1993). James and Savage (1990) used recordings at a single seismic station of multiple microearthquake sources to identify crustal reflectors at depths of 10-11 km and 13-14 km beneath the Big Island of Hawaii. In that study, 20 events were source migrated to remove the effects of varying focal depths (James and Savage, 1990).

Microearthquakes were recorded during the SEA-CALIPSO deployment from Dec 17, 2007 through Dec 20, 2007. A total of twenty local events were identified from the continuous data recording from these three days and correlated with events located by Miller *et al*. (2008) from the areal seismic network on Montserrat. Locations were made with HypoEllipse (Lahr, 1999) by using a multi-layer 1-D approximation of the SEA-CALIPSO velocity model developed by Shalev *et al*. (2010). The epicenters were centered near the summit of SHV at relatively shallow depth, thus providing near vertical reflection coverage for depth points relatively close to SHV (Figure 13). The microearthquakes were treated in the same manner as borehole shots in a

conventional controlled source profile. Although these events were recorded along all three profiles, attention here is focused on those associated with the Belham Valley line, as they sample most closely to the SHV (Figure 13).

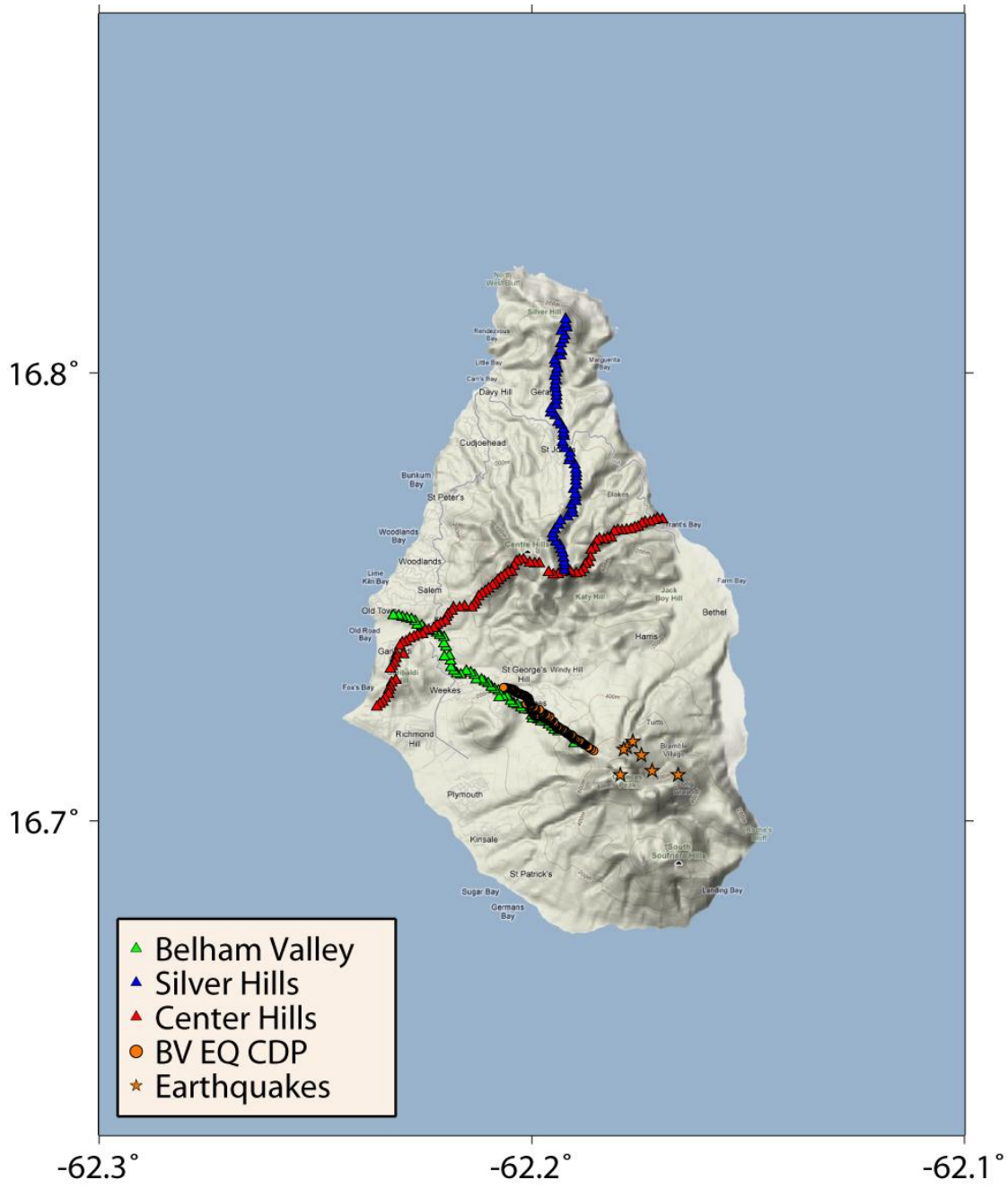

Figure 13 - Map showing geophone locations, earthquake locations and the earthquake CDP locations for the Belham Valley line.

One challenge using natural sources is the inherent uncertainty in the location and origin times of the sources. To reduce the influence of inaccuracies in depth, particularly for stacking purposes, the events were separated into three different groups based upon reported precision in the location. For events that had a horizontal location error less than one kilometer, the reported location was accepted for processing purposes. The seven events in this category (A) are shown explicitly in Figures 1 and Table 1.

Table 1 - List of microearthquakes in category A, their origin times and locations.

Event	Origin Time	Latitude	Longitude
1518	2007.351.23.02.40.97	N16°43.07’	W62°10.60’
2146	2007.352.10.50.39.58	N16°42.65’	W62°10.77’
2252	2007.352.12.36.10.16	N16°42.88’	W62°10.48’
2254	2007.352.12.38.37.90	N16°42.62’	W62°09.97’
2361	2007.352.14.28.51.85	N16°42.67’	W62°10.33’
2363	2007.352.14.30.48.49	N16°42.99’	W62°10.68’
2579	2007.352.18.06.30.42	N16°42.96’	W62°10.73’

Events with horizontal location errors greater than one kilometer but less than 2.5 kilometers were grouped together as category B. An average location was used for processing these seven events. Events with horizontal location errors greater than 2.5 kilometers were assigned to category C. The six events in this category were visually inspected for consistency with the other earthquake recordings, but were not used joint processing due the relatively large location uncertainties.

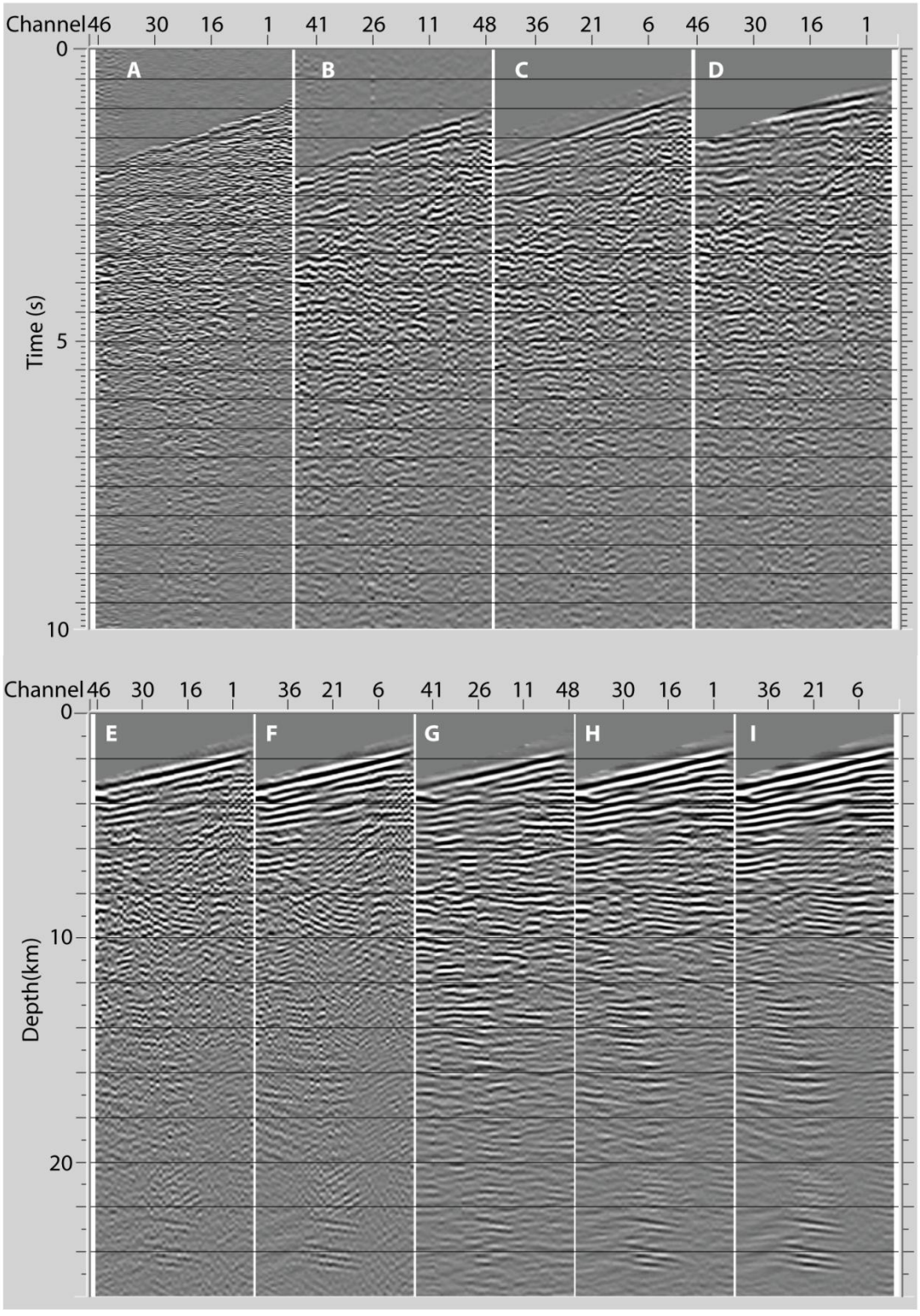

Figure 14- Effects of processing. A. raw data B. data with bandpass filter C. Aligning on first arrival D. NMO E. FX-decon F. FX-decon twice G. Trace mix H. FX-decon and trace mix I. FX-decon twice and trace mix.

The raw earthquake gathers (e.g. Figure 14) all show clear indications of organized energy that cannot be attributed to direct P, S or surface wave energy, but rather suggest moveout consistent with reflected arrivals. However, individual reflections are difficult to trace undisrupted across the array, which we suspected was due to relative “static” shifts associated with the overlying crust. Several processing steps were used to enhance signal coherency of potential reflected energy. These steps are illustrated in Figure 14.

The data were cut so t=0 is the origin time of the earthquake. Starting with the raw data, elevation statics were applied to correct for changes in topography along the seismic lines, then the data were bandpass filtered from 1 to 8 Hz. To further improve reflection coherence, we applied a form of refraction statics. First P wave arrivals were aligned to near -horizontal using linear moveout (LMO) corrections. Deviations of the first arrival time from horizontal were manually picked and used to apply a static shift to force alignment of the first arrival. The LMO correction was subsequently removed, hopefully with increased lateral alignment of reflections as well as first arrivals. A normal moveout correction (NMO) was then applied using an average velocity of 5km/s from 0s to 10s to image reflection geometry at depth. Several additional coherency enhancement techniques were used to further increase the visibility of reflected energy and the two that appeared to best enhance the data were FX-deconvolution and trace mixing. Various combinations of these two routines were applied to find the combination that best improved the visual coherency of the reflectors. Of the various combinations, the most effective appeared to be application of FX-deconvolution twice followed by a single trace mix (Figure 14).

As cited above, seven of the recorded microearthquakes provided locations with particularly low error estimates. However, due to technical issues with the recording equipment on the Belham Valley line for a portion of the survey, not all of the data for all seven events were recovered. In spite of this loss, the processed gathers for all seven events (Figure 15) show striking similarities despite being recorded for different earthquake sources. Note that the microearthquake gathers in Figure 15 are displayed in depth using a provisional average upper crustal velocity of 5km/s.

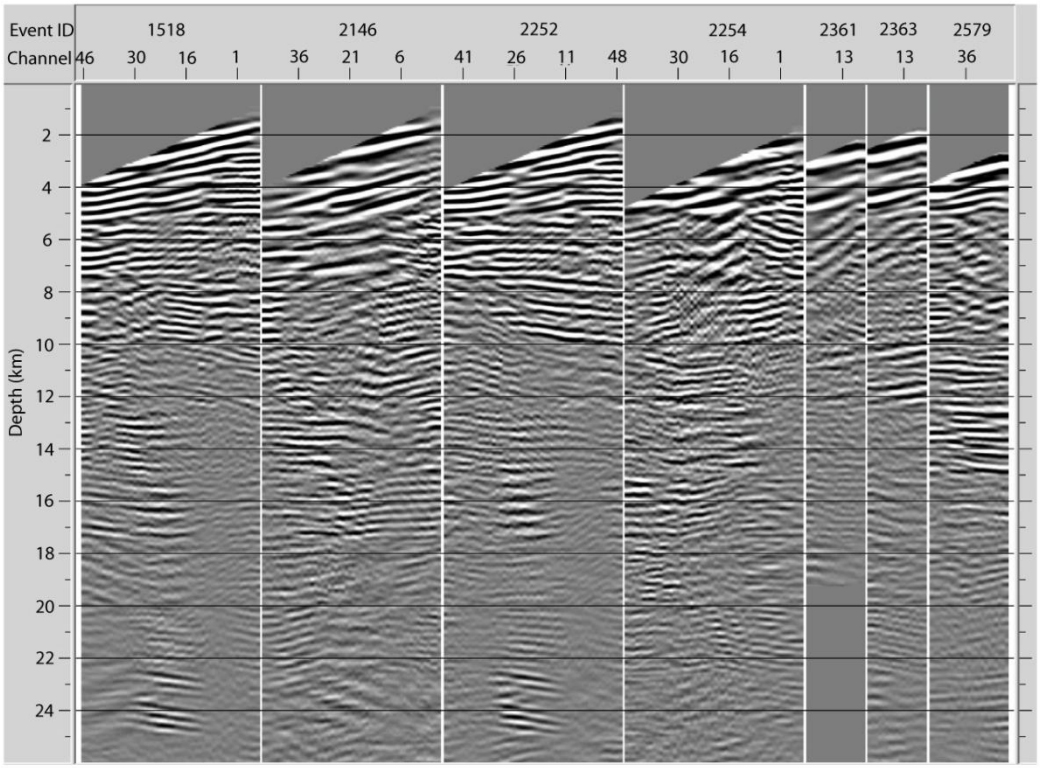

Figure 15 - Source gathers for the 7 best located earthquakes, as recorded along the Belham Valley line. Differences in the number of traces in each gather are due to failure of a subset to the array to operate during this time period.

Before addressing the interpretation of the apparent reflectivity on these gathers, we must consider the potential artifacts that are inherent in such heavy use of algorithms such as FX-decon and trace mixing. This combination can be expected to emphasize sub-horizontal energy versus dipping energy, and linear events versus curved events (e.g. diffractors). There are certainly indications of diffractions from, presumably, small bodies (intrusions) on some of the unprocessed shot gathers around 1 to 2 seconds (e.g. Figure 14). A more serious concern is that the heavy use of these multichannel filters are generating spurious coherence out of background "noise" or very weak arrivals (direct or multiple) from the airgun sources. To assess these possibilities, we processed "background" gathers consisting of data from the minute preceding and the minute following the 60 second interval beginning with the origin time of a sample earthquake. These "noise" gathers were then processed with exactly the same sequences and parameters used for the earthquake record they bracket. These gathers contain a similar signal from the airgun that would appear on the earthquake record, but for our purposes the gathers would be considered "noise". These "noise" gathers were then processed in the exact same way as the corresponding earthquake using the FX-decon and the trace mix, and compared in true amplitude format with the earthquake gathers.

Figure shows two independent earthquakes recordings along with their bracketing "noise" intervals. Note that each earthquake (shaded section) occurs at a different time relative to the shot time (t=0) for each window: earthquake 1518 occurs ~40s after the first arrival of the shot, while earthquake 2252 occurs ~10s after the first arrival of the shot. The identically processed versions of these datasets are shown in Figure B. The two

processed earthquakes gathers look very similar, with several coherent features at similar depths exhibiting similar dips, in particular at 3-4 sec, 6-7 sec and 9-10 sec. Given that the earthquake origin times lag behind the shot times (t=0) so differently in these two cases, it is difficult to attribute common "reflections" to enhanced arrivals of airgun energy. Certainly the amplitudes of the coherent events on the earthquake gathers are substantially larger than any coherence within the processed noise gathers. An exception occurs for earthquake 2252, where there seems to be a coherent arrival at 2-4 sec on both the earthquake gather and the "trailing" noise gathers. However, in this case the earthquake origin time is very close to the airgun shot time, so that processing may be enhancing energy from both sources at the same time. In general however, the earthquakes do not occur so close to the arrival of energy from the airgun sources (Figure 17).

Figure 16 - A: Earthquake gathers for events 1518 and 2252 with adjacent "noise" gathers. B: Earthquake and noise gathers for the shaded regions in A

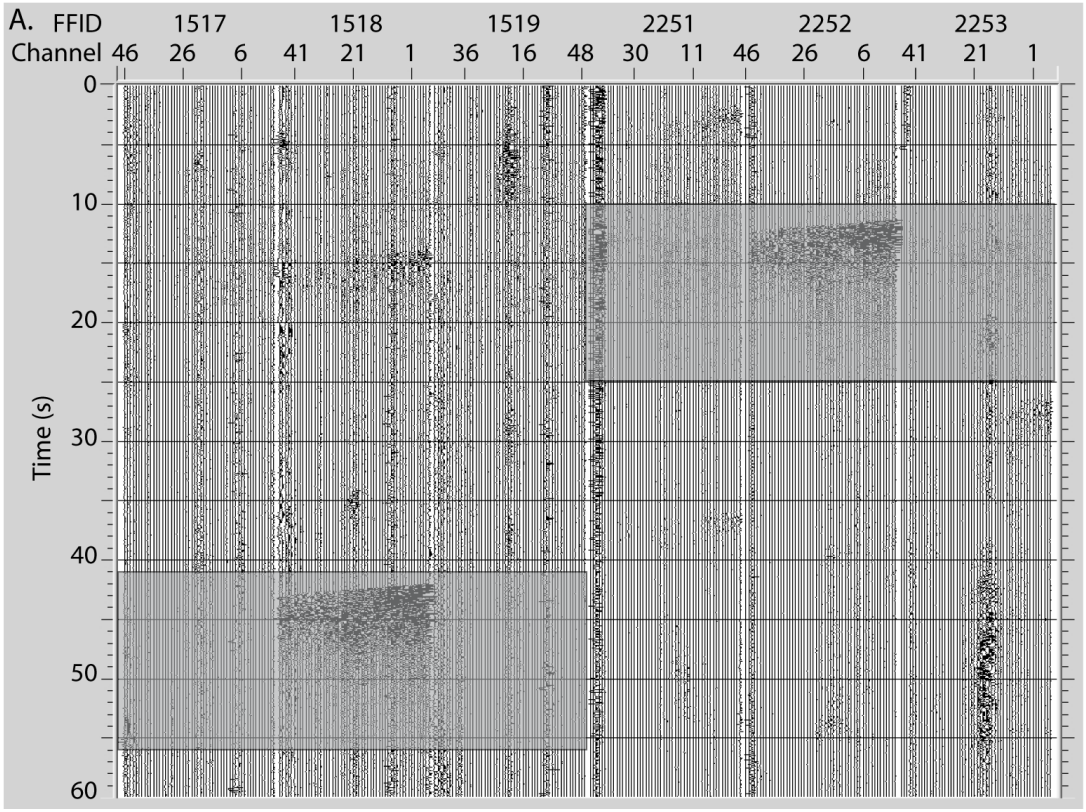

Figure 16 - A: Earthquake gathers for events 1518 and 2252 with adjacent "noise" gathers. B: Earthquake and noise gathers for the shaded regions in A.

Figure 16 Continued

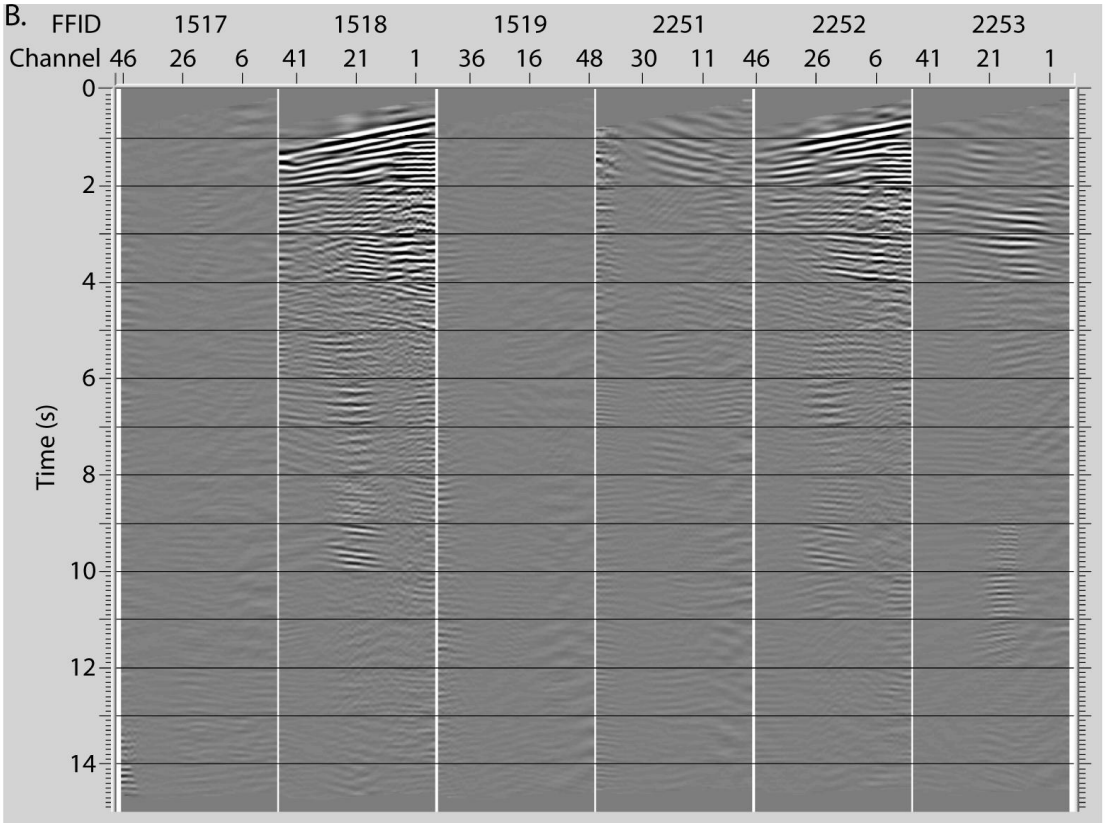

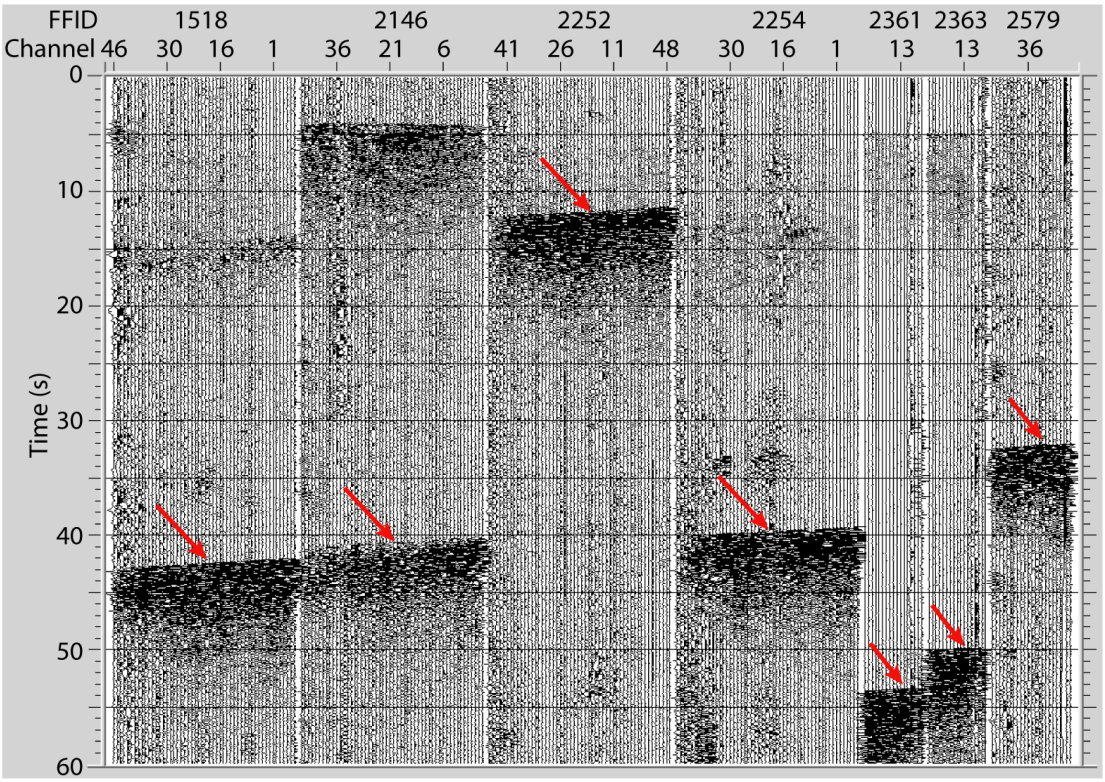

Figure 17 - Earthquake arrivals shown in relation to the shots. Earthquake arrivals are highlighted with a red arrow.

Most of the processing described above focused on signal enhancement within individual source gathers (Figure 14, 17). We also attempted to “stack” the Belham Valley recordings for several of the earthquakes. Because of lateral scatter in the reported locations of the microearthquake sources, which results in lateral dispersal of the common reflecting points (Figure 18), we restricted our stack to those events whose common reflections points were close to co-linear. The resulting low fold (up to 5) stack is shown in Figure 19, with and without coherency enhancement and in comparison to an individual shot gather.

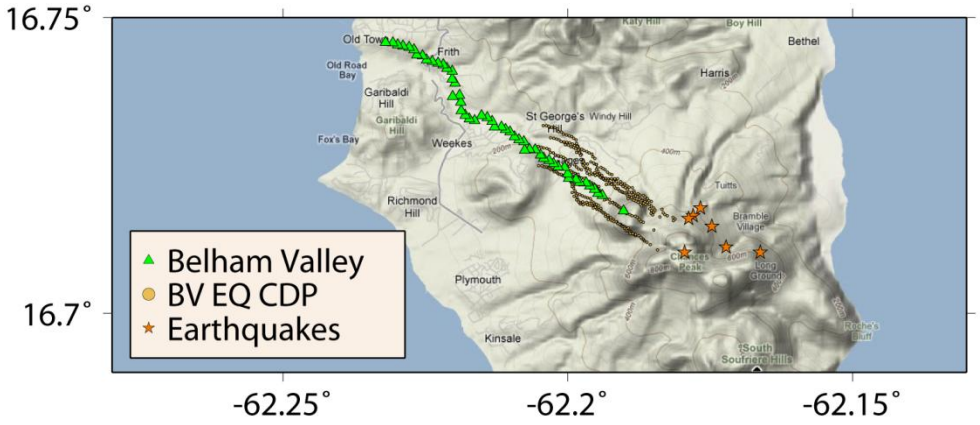

Figure 18 - Map showing the scattered locations of the CDPs for the microearthquakes and the Belham Valley line.

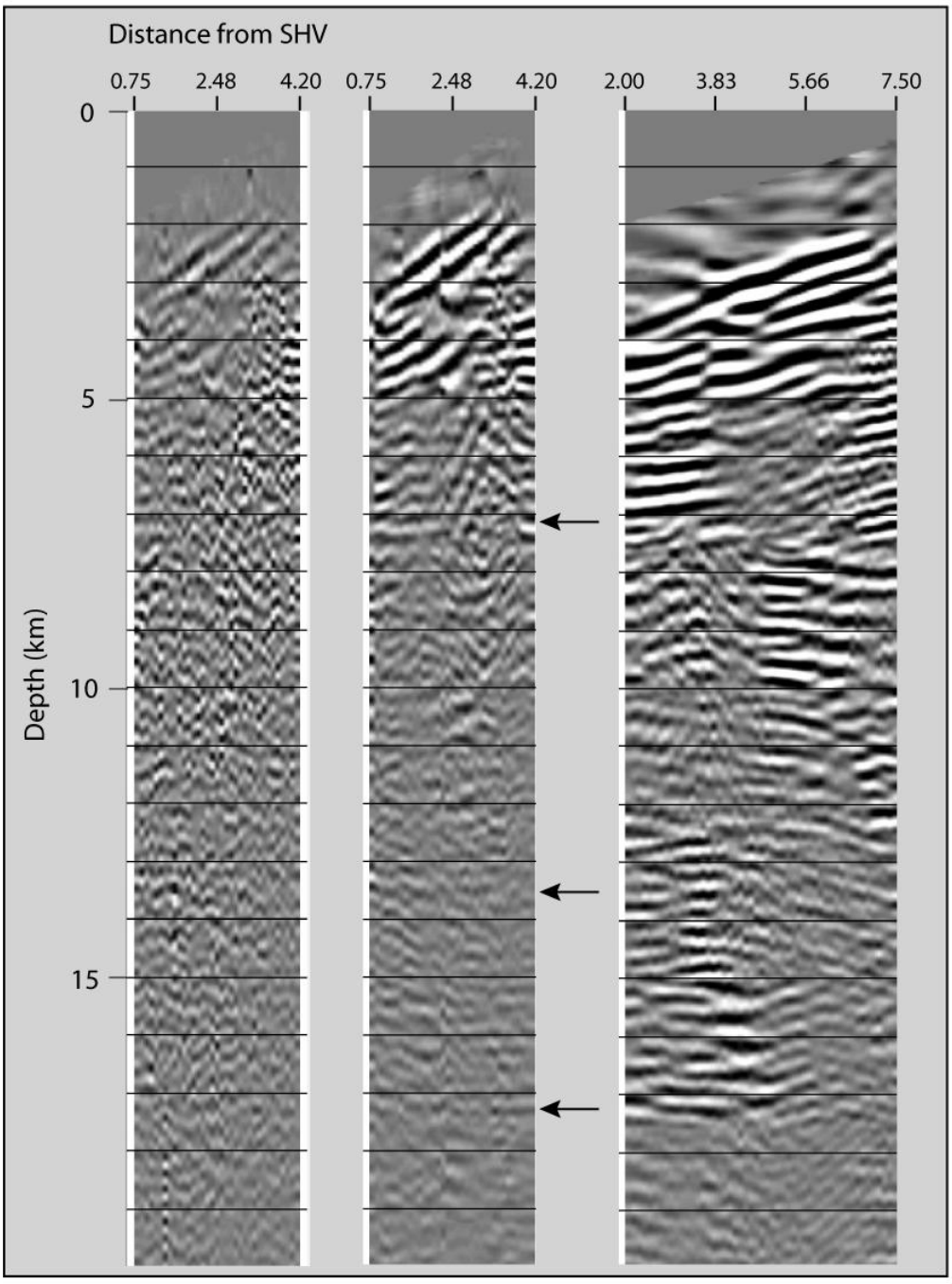

Figure 19 - CDP stack for the Belham Valley line. Left: No coherency filter Middle: FX-decon x 2 plus trace mixing Right: individual earthquake gather with FX-decon x 2 plus trace mixing. Arrows indicate possible reflections.

Given the uncertainty in source locations and the low redundancy (fold) it is not surprising that the stack shows little, if any, coherency improvement relative to the gathers. This exercise is perhaps more useful as a feasibility demonstration that CMP methods can be applied to microearthquake recordings, but emphasizing the need for many more sources and better source locations.

The microearthquakes were also recorded on the other two lines, Silver Hills (Figure 20) and Centre Hills (Figure 21), though some of the smaller events were of lower quality due to the larger source-receiver offset. The earthquakes on these lines were processed identically to the data from Belham Valley. Sections using the same event were created to show a comparison between the three lines to look for common features (Figure 22). The gathers from the Silver Hills and Centre Hills lines showed some similarities to the Belham Valley line and to each other. There are possible common reflectors between 3 to 4 seconds and 5 to 6 seconds. These could correspond to layering found throughout the entire island.

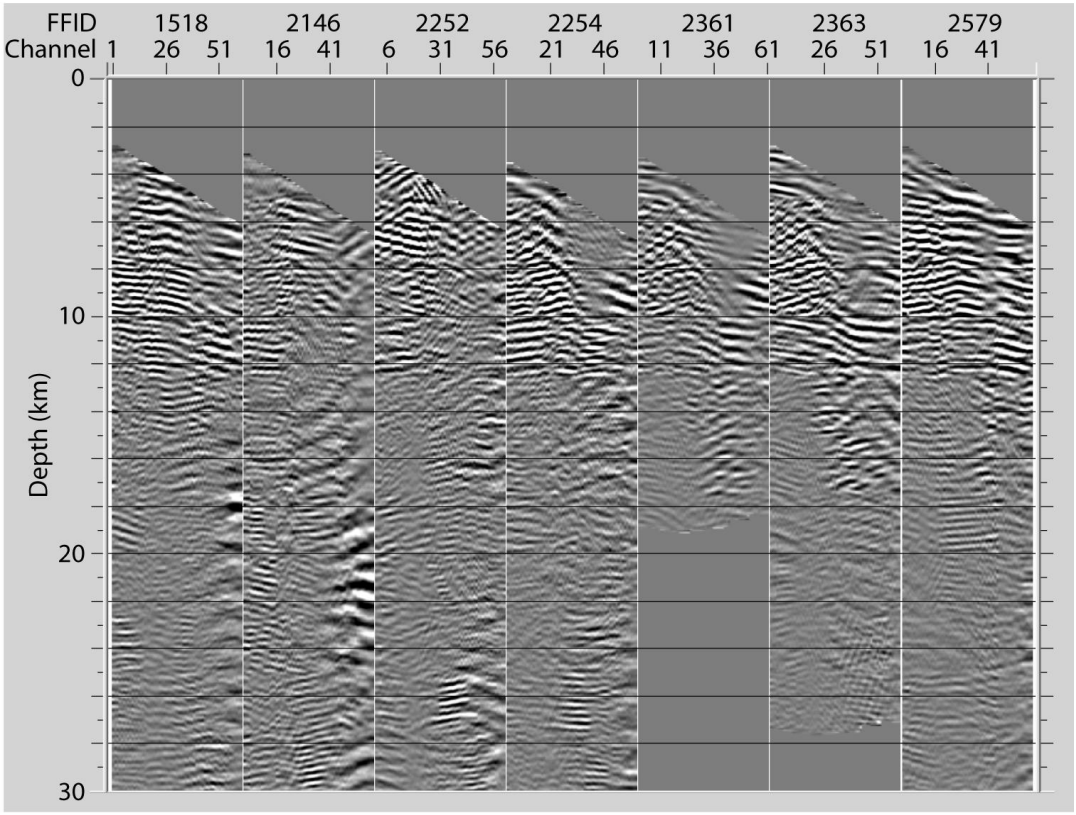

Figure 20 - Seven best earthquake gathers from the Silver Hills line

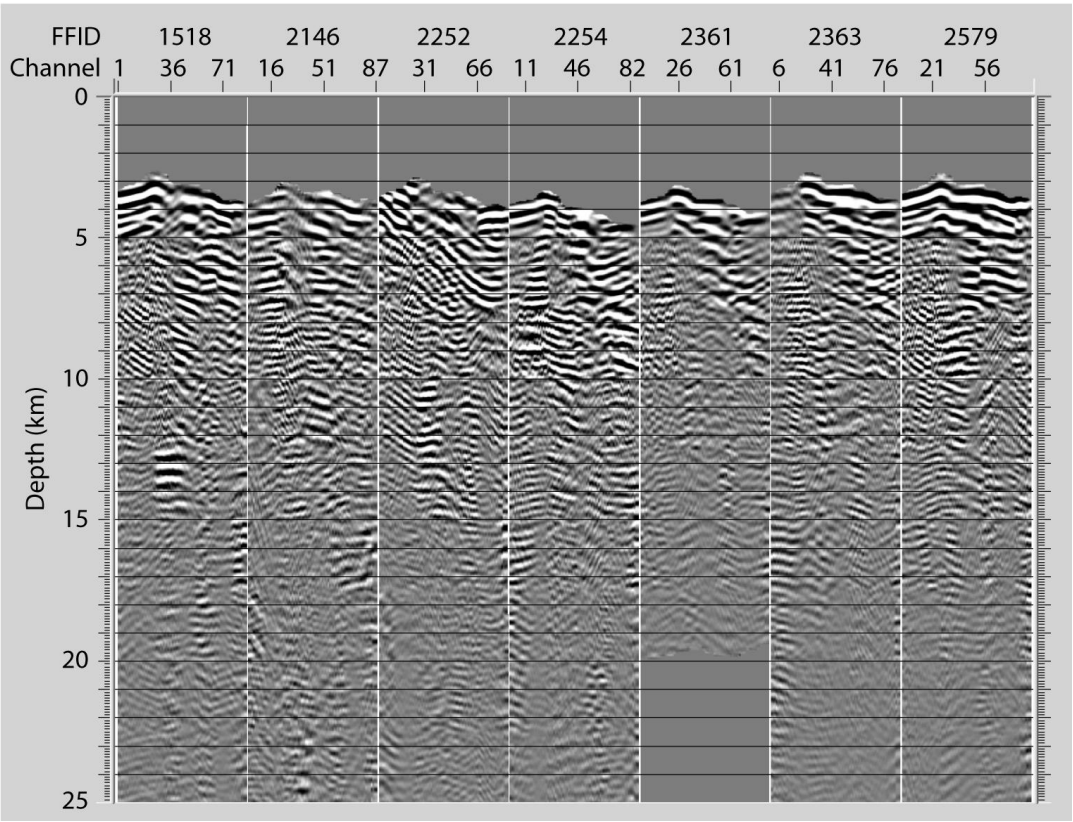

Figure 21 - Seven best earthquake gathers for the Centre Hills line.

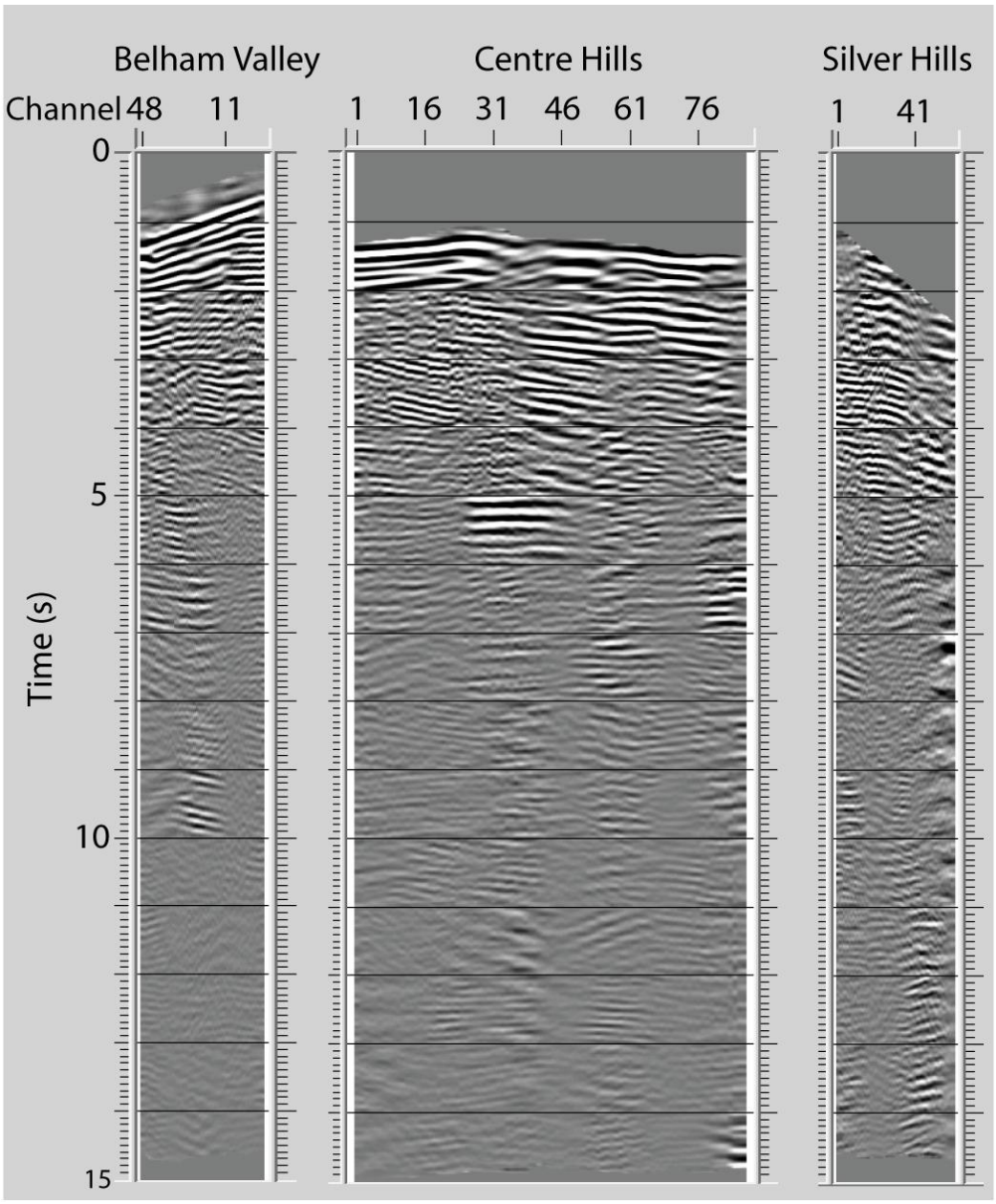

Figure 22 - Comparison of one earthquake as recorded on all 3 lines (source gathers).

Comparison to controlled source data

After the success we had processing the earthquake data in the specific fashion describe above, we tried processing the shot data for the Belham Valley line identically to the earthquake data. This would allow for the

comparison between the shot gathers on the Belham Valley line and the earthquake records. The shot gathers we choose to process in this manner are along a radial line to the Belham Valley line and the microearthquakes used for this study are also located along this line (Figure 23). The shots used here are among the closest to the geophones that would sample the structure beneath SHV. There are no reflections on the airgun data without the coherency processing that look convincing (Figure 24). However the same gathers with the coherency processing appear to have possible reflectors (Figure 25). This is especially apparent around 20km where a similar event is found on all the gathers (Figure 25). The redundancy of having this event on all four gathers improves its believability as a possible reflector rather than the coherency processing enhancing noise. There is also a possible event at a depth of 27km found on two of the gathers shown here (Figure 25). It may not be observed on the other gathers due to the difference in location of the airgun shots.

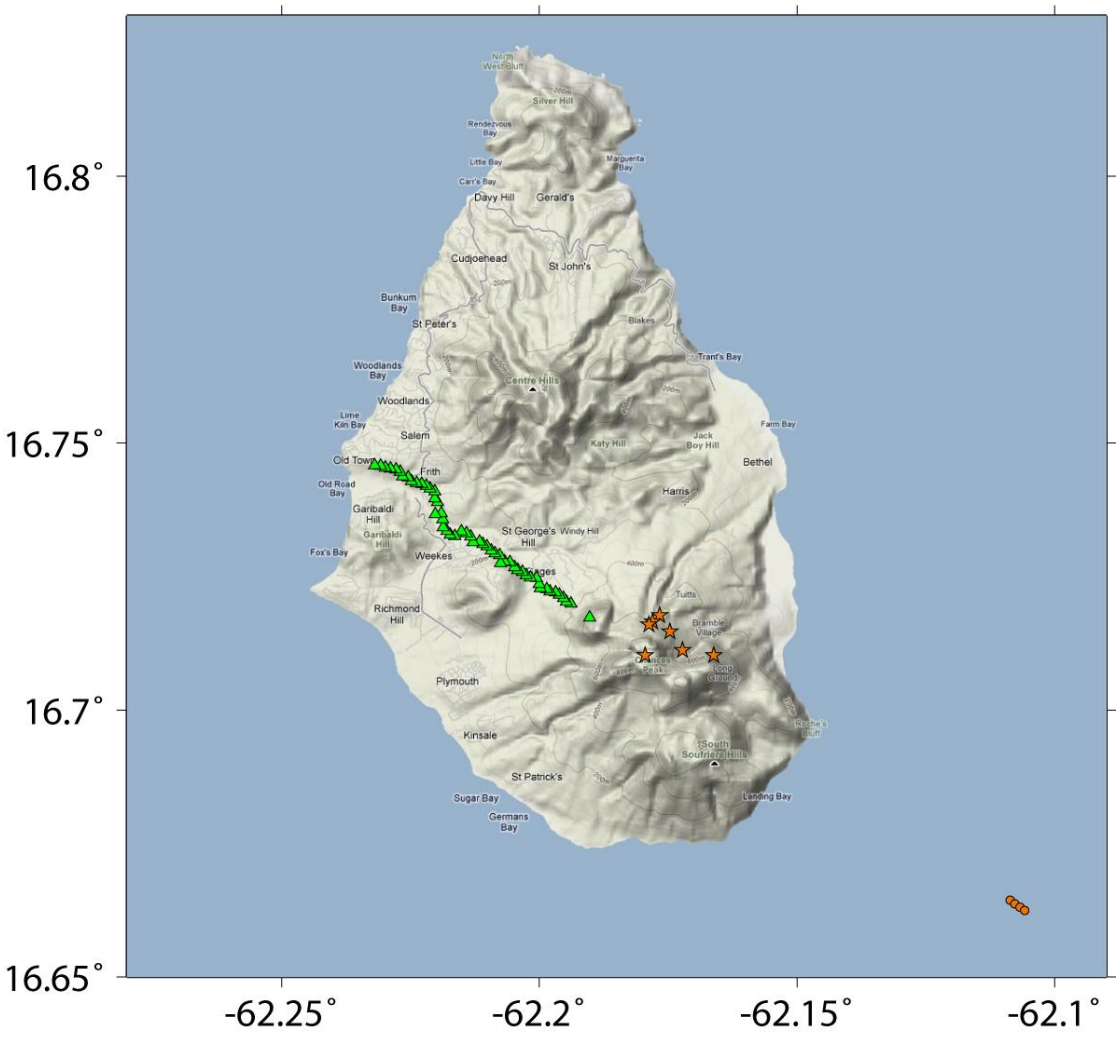

Figure 23 - Map showing the comparison shots in relation to the earthquakes and the Belham Valley stations.

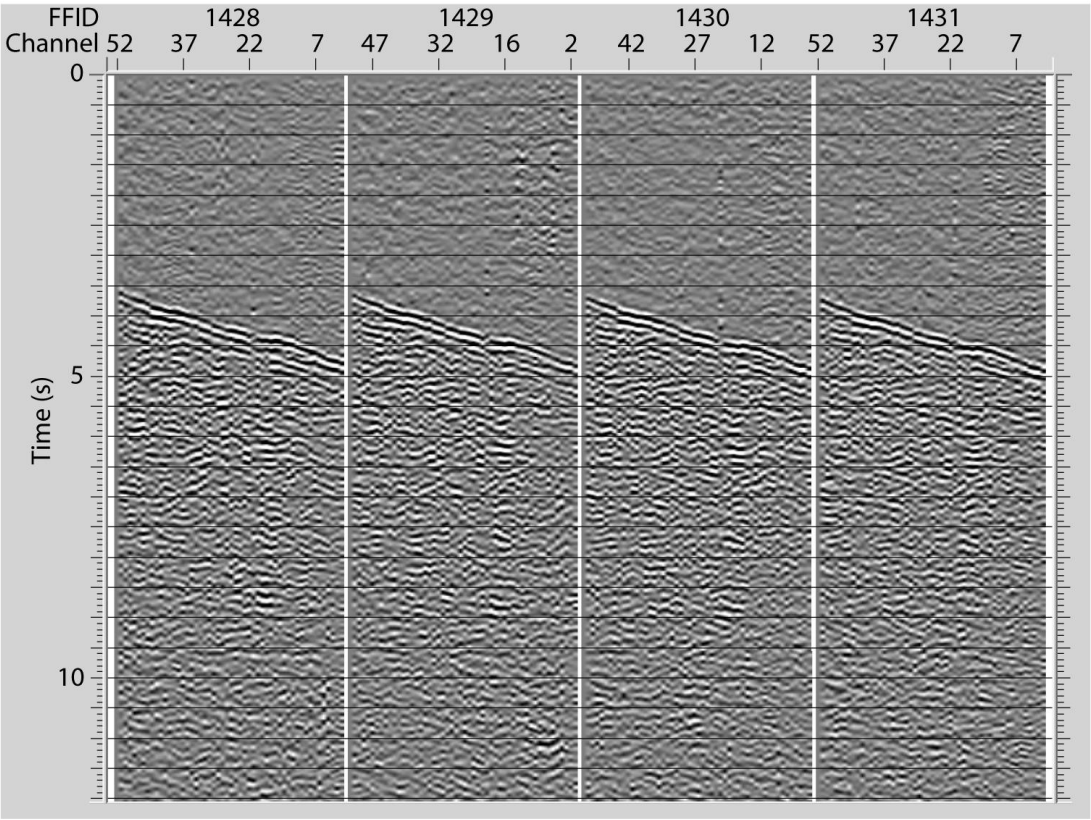

Figure 24 - Shot gathers for test subset with no coherency processing

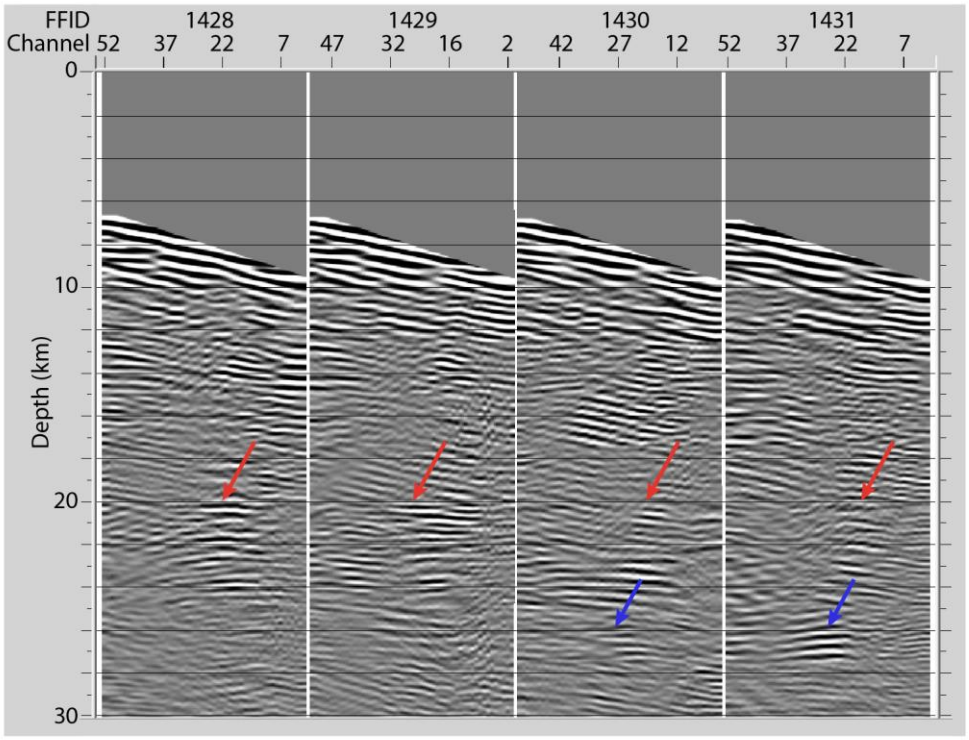

Figure 25 - Shot gathers with coherency processing, converted to depth (including correction for water depth beneath airgun). Arrows point to possible reflections

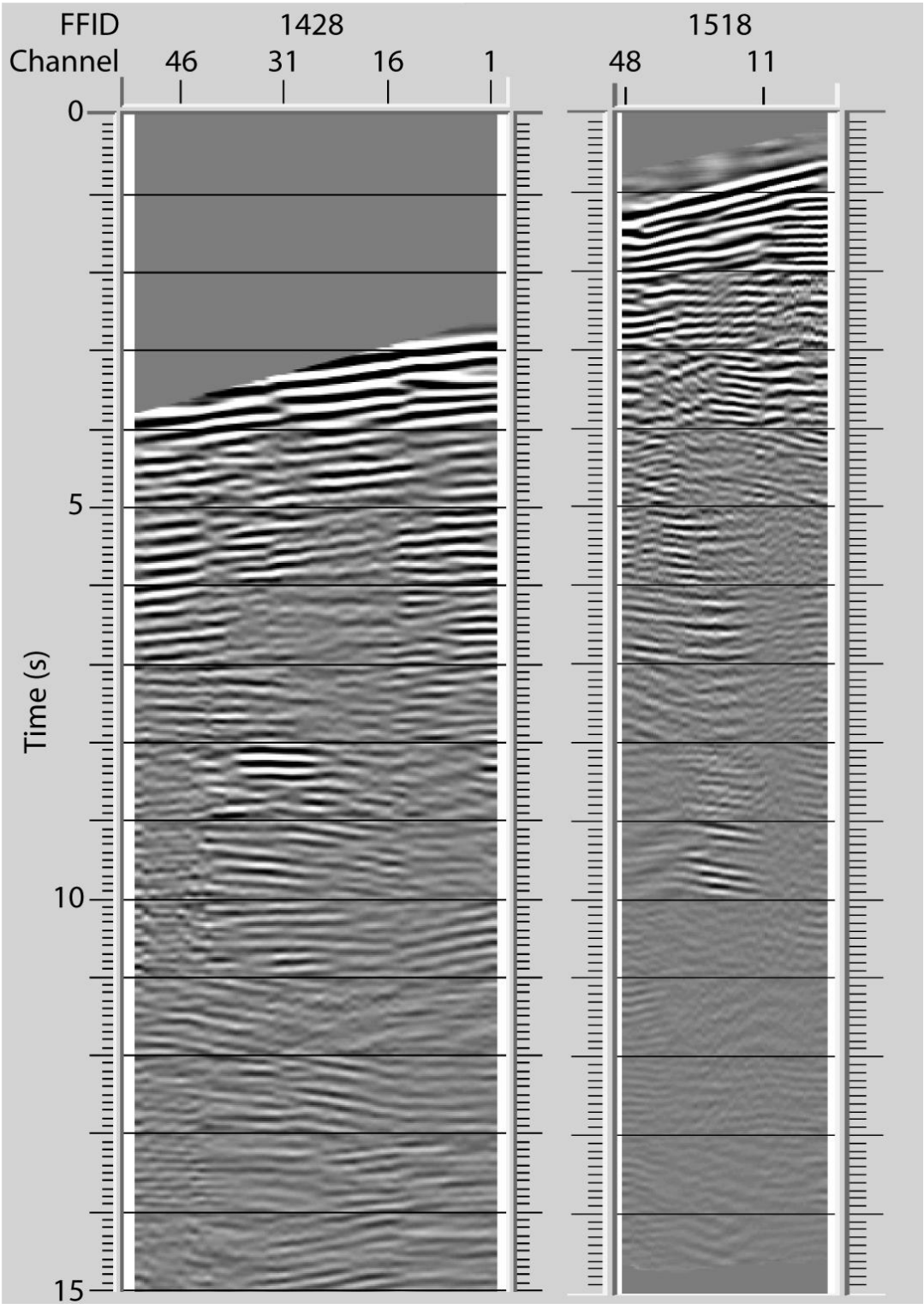

Figure 26 - Comparison between an airgun shot (left) and earthquake (right) gather processed with coherency enhancement.

Although the shots gathers are not as detailed in the shallow subsurface structure for the reasons discussed above, there are some obvious similarities between the earthquake records and the shot gathers (Figure 26). The biggest similarity is the feature that is located at ~9.5 seconds. This shows up on two of the earthquake records and several of the shot gathers. This time is slightly different than the times that this feature shows up at on the microearthquake records, but this could be due to variations in the wave path that were not taken into account in the model used to convert time to depth. While we did factor in the delay that the waves from the shot would face going through the water column, the energy from the shots also traveled through the oceanic crust, while the energy from the microearthquake did not. The differing depths of the shots and the microearthquakes have not been taken into account, which could account for slight differences in depth to reflectors. Another possibility is there are real variations in the depth to this reflector over the different distances being imaged.

Interpretation

The individual earthquake gathers from the Belham Valley line (Figure 15) show consistent subhorizontal energy between 6 and 19 km depth beneath the NW flank of Soufriere Hills Volcano. On the Belham Valley CDP stack (Figure 19), the stronger reflectors are at similar depths as the reflectors seen on the individual gathers. However, as they are such low amplitude that they need considerable enhancement just to be visible, it is difficult to argue that they mark fluid bodies at depth. It could be argued that intrinsic attenuation in the crust near SHV might render even a “bright spot” reflection as relatively weak arrival, but this is mere speculation. Given the quality of the

unprocessed data, attempts to identify the polarity of these reflectors have been unfruitful. We are thus left with the likelihood that these reflectors represent buried volcanic layering and or later intrusion of sills into the crustal edifice. Comparison with crustal data from teleseismic studies (Sevilla *et al*, 2008) suggest that neither of these reflections correspond to the Moho.

Conclusion

The presence of sill-like features in the upper crust beneath an active volcano is not surprising. The primary value of this study, we would argue, is its demonstration that relatively high resolution reflection imaging of crustal structure is feasible using microearthquake sources. In regions near active volcanoes, like SHV, placement of controlled sources near the summit, as required to obtain near vertical illumination of subvolcanic structure, is problematic at best. Microearthquakes offer an alternative in such situations, requiring only dense array recording in continuous mode over long periods of time (compared, at least, to a typical controlled source survey). As we have shown, the data can be processed with conventional reflection techniques. The efficacy of this approach, however, is dependent upon the quality of relative event locations and the number and distribution of such sources in space.

REFERENCES

Aspinall, W.P., A.D. Miller, L.L. Lynch, J.L. Latchman, R.C. Stewart, R.A. White, and J.A. Power, (1998), Soufriere Hills eruption, Montserrat, 1995-1997. Volcanic earthquake locations and fault plane solutions, *Geophys. Res. Lett.*, 25 (18),3397-3400.

Balch, R., H. Hartse, A. Sanford, and K. Lin (1997), A new map of the geographic extent of the Socorro midcrustal magma body, *Bull. Seismol. Soc. Amer*., *87*, 174-182

Barclay, J., Rutherford, M.J., Carroll, M.R., Murphy, M., Devine, J.D., Gardner, J., and Sparks, R.S.J., (1998), Experimental phase equilibria constraints on pre-eruptive storage conditions of the Soufriere Hills magma, *Geophys. Res. Lett.*, 25, 3437-3440.

Brown, L. D., P. A. Krumhansl, C. E. Chapin, A. R. Sanford, F. A. Cook, S. Kaufman, J. E. Oliver and F. S. Schilt (1979), COCORP seismic reflection studies of the Rio Grande Rift, in *Rio Grande Rift; tectonics and magmatism,* edited by R.E. Riecker, 169-184, AGU, Washington, D.C.

Brown, L. D., W. Zhao, K. D. Nelson, M. Hauck, D. Alsdorf, A. Ross, M. Cogan, M. Clark, X. Liu and J. Che (1996), Bright spots, structure, and magmatism in southern Tibet from INDEPTH seismic reflection profiling, *Science, 274*(5293), 1688-1690.

Chmielowski, J., G. Zandt, and C. Haberland (1999), The Central Andean Altiplano- Puna Magma Body, *Geophys. Res. Lett., 26* (6), 783-786.

de Voogd, B., L. Serpa, L. Brown, E. Hauser, S. Kaufman, J. Oliver, B. W. Troxel, J. Willemin and L. A. Wright (1986), Death Valley bright spot; a midcrustal magma body in the southern Great Basin, California?, *Geology*, *14*(1), 64-67.

Elsworth, D., G.S. Mattioli, J. Taron, B. Voight, R. Herd, (2008), Implications of magma transfer between multiple reservoirs on eruption cycling, *Science*, 322, 246-248.

Hasegawa, A., D. Zhao, S. Hori, A. Yamamoto and S. Horiuchi, 1991, Deep structure of the northeastern Japan arc and its relationship to seismic and volcanic activity, *Nature, 352,* 683 – 689. doi:10.1038/352683a0.

Harford, C.L., M.S. Pringle, R.S.J. Sparks, and S.R. Young, (2002), The volcanic evolution of Montserrat using 40 Ar/ 39 Ar geochronology. in *The Eruption of Soufriere Hills Volcano, from 1995 to 1999 (T.H.Druitt and B. Kokelaar, eds.), Geological Society of London, Memoirs*, 21, 45-69.

Iidaka, T., K. Miura and A. Ikami (1993), Evidence for the existence of a mid-crustal reflector in the Beppu-Shimabara Graben, Kyushu, Japan, *Geophys. Res. Lett.*, *20* (16), 1699-1702.

Inamori, T., S. Horiuchi and A. Hasegawa (1992), Location of mid-crustal reflectors by a reflection method using aftershock waveform data in the focal area of the 1984 western Nagano Prefecture earthquake, *J. Phys. Earth*, *40* (2), 379-393.

James, D. E. and M. K. Savage (1990), A search for seismic reflections from the top of the oceanic crust beneath Hawaii, *Bull. Seismol. Soc. America, 80* (3), 675-701.

Lahr, J. C. (1999) , HYPOELLIPSE; a computer program for determining local earthquake hypocentral parameters, magnitude, and first-motion pattern (Y2K compliant version), Open File Report, U.S. Geological Survey**.**

Mattioli, G.S., T.H. Dixon, F. Farina, E.S. Howell, P.E. Jansma, and A.L. Smith, (1998), GPS measurement of surface deformation around Soufriere Hills Volcano, Montserrat from October 1995 to July 1996, *Geophys. Res. Lett.*, 25 (18), 3417-3420.

Miller, V., C. Ammon, B. Voight, S. De Angelis (2008), Source Mechanisms of High-Frequency-Onset Earthquakes Recorded Beneath Soufriere Hills Volcano, Montserrat, During SEA-CALIPSO Deployment, Oct-Dec 2007, *Eos Trans. AGU, 89*(53), Fall Meet. Suppl., Abstract V51C-2041

Paulatto, M., T. A. Minshull, B. Baptie, S. Dean, J. O. S. Hammond, T. Henstock, C. L. Kenedi, E. J. Kiddle, P. Malin, C. Peirce, G. Ryan, E. Shalev, R. S. J. Sparks and B. Voight, (2010), Upper crustal structure of an active volcano from refraction/reflection tomography, Montserrat, Lesser Antilles*. J. Geophys. Int,* 180 (2), 685-696.

Sanford, A.R., and L.T. Long (1965), Microearthquake crustal reflections, Socorro, New Mexico, *Bull. Seismol. Soc. Amer.*, *55*, 579-586.

Sanford, A. R., O. Alptekin and T. R. Toppozada (1973), Use of reflection phases on microearthquake seismograms to map an unusual discontinuity beneath the Rio Grande Rift, *Bull. Seismol. Soc. Amer*., *63* (6), 2021-2034.

Sanford, A. R., R. P. Mott, Jr., P. J. Shuleski, E. J. Rinehart, F. J. Caravella, R. M. Ward and T. C. Wallace (1977), Geophysical evidence for a magma body in the crust in the vicinity of Socorro, New Mexico, in *The Earth's crust; its nature and physical properties,* edited by J.G. Heacock etl., *Amer. Geophys. Union Geophys. Monogr,*, *20*, 385-403.

Sevilla, W., C. Ammon, V. Miller, B. Voight (2008), Teleseismic Imaging of Crustal Structure and Magma Storage Regions Beneath Montserrat, *Eos Trans. AGU, 89*(53), Fall Meet. Suppl., Abstract V51C-2040.

Shalev, E., et al. (2010), 3-D Seismic velocity tomography of Montserrat from the SEA-CALIPSO offshore/onshore experiment. *Geophys. Res. Lett., Special Section on Montserrat.*

Sheetz, K. E. and J. W. Schlue (1992), Inferences for the Socorro magma body from teleseismic receiver functions, *Geophys. Res. Lett., 19* (18), 1867-1870.

Shepherd, J.B., J.F. Tomblin, and D.F. Woo, (1971), Volcano-seismic crisis in Montserrat , West Indies, 1966-67: *Bulletin Volcanologique*, 35, 143-163.